Contribution from the Department of Chemistry and Molecular Structure Center, Indiana University, Bloomington, Indiana 47405

Reactions of Metal–Metal Multiple Bonds. 15.[1] Reactions of $M_2(OR)_6(M{\equiv}M)$ Compounds (M = Mo, W) with 9,10-Phenanthrenequinone and Tetrachloro-1,2-benzoquinone

Timothy P. Blatchford, Malcolm H. Chisholm,* and John C. Huffman

Received April 7, 1987

$Mo_2(OR)_6$ compounds, where R = *i*-Pr and *neo*-Pe (*neo*-Pe = neopentyl), and $W_2(O\text{-}i\text{-}Pr)_6L_2$, where L = pyridine and $HNMe_2$, react in hydrocarbon solvents with either 9,10-phenanthrenequinone or tetrachloro-1,2-benzoquinone to generate $M_2(OR)_6(OO)_2$, $M_2(OR)_3(OO)_3$, and $M_2(OR)_2(OO)_4$ compounds in a sequential manner, where OO represents the fully reduced form of the quinone ligand, i.e. catecholate. Though it has not proved possible to isolate each member of the series in a pure state, at least one compound from the series has been fully characterized by a single-crystal X-ray study. In these reactions the $(M{\equiv}M)^{6+}$ unit is oxidized to $(M{-}M)^{10+}$ and every product contains a M—M single bond supported by a pair of bridging alkoxide ligands. Each molybdenum atom is in a distorted-octahedral environment with respect to a set of six oxygen atoms and the M–M distances are in the range 2.7–2.8 Å. ^1H NMR spectra are generally supportive of the structures found in the solid state, though for $M_2(OR)_4(OO)_3$ compounds temperature-dependent behavior indicative of stereochemical lability is observed. The reaction between $Mo_2(O\text{-}t\text{-}Bu)_6$ and tetrachloro-1,2-benzoquinone (2 equiv) is more drastic in regard to the decomposition of the alkoxide ligand. By the subsequent addition of pyridine (py) the red crystalline salt $[pyH]_2[(MoO_2(O_2C_6Cl_4)py)_2O]$ has been isolated and shown to contain two *cis*-MoO_2^{2+} units linked by an oxo bridge. Crystal data: (i) $Mo_2(O\text{-}i\text{-}Pr)_6(O_2C_6Cl_4)_2$ at −160 °C, a = 10.579 (5) Å, b = 11.014 (5) Å, c = 9.619 (4) Å, α = 108.38 (2)°, β = 108.44 (2)°, γ = 84.49 (2)°, Z = 1, d_{calcd} = 1.711 g cm^{-3}, space group $P\bar{1}$; (ii) $Mo_2(O\text{-}neo\text{-}Pe)_6(O_2C_6Cl_4)_2$ at −160 °C, a = 11.826 (7) Å, b = 14.176 (10) Å, c = 17.682 (12) Å, β = 96.34 (3)°, Z = 2, d_{calcd} = 1.353 g cm^{-3}, space group $P2_1/c$; (iii) $Mo_2(O\text{-}i\text{-}Pr)_4(O_2C_{14}H_8)_3{\cdot}2THF$ at −163 °C, a = 18.520 (10) Å, b = 13.76 (6) Å, c = 12.920 (6) Å, α = 114.69 (3)°, β = 110.56 (2)°, γ = 71.97 (3)°, Z = 2, d_{calcd} = 1.446 cm^{-3}, space group $P\bar{1}$; (iv) $[pyH]_2[(MoO_2(O_2C_6Cl_4)_2py)_2O]$ at −162 °C, a = 31.613 (15) Å, b = 13.365 (4) Å, c = 18.207 (6) Å, β = 92.27 (2)°, Z = 8, d_{calcd} = 1.880 g cm^{-3}, space group $P2_1/c$.

Introduction

o-Quinone and its substituted derivatives have found an extensive coordination chemistry based on oxidative-addition reactions,[2] their relevance to metal-catalyzed biological redox reactions of quinones[3] and quinoid molecules,[4] and analogy with the interesting chemistry of 1,2-dithiolene systems.[5] The coordination chemistry of *o*-benzoquinone ligands has been the subject of a recent review.[6]

Catecholates, *o*-semiquinones, and *o*-benzoquinones are related by the addition or removal of charge (eq 1). Electrochemical

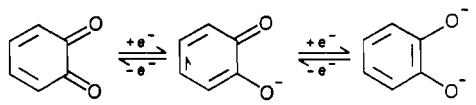

(1)

interconversion of these forms can occur via one- or two-electron processes.[7] As might be expected, transition-metal complexes containing *o*-benzoquinone ligands are rich in redox chemistry, exhibiting a wide range of oxidation states.[8] *o*-Benzoquinones are "noninnocent ligands", and the determination of the oxidation state of the metal and the ligands in these complexes is often difficult.

Oxidation states for ligands and metals in these compounds have usually been assigned on the basis of carbon–oxygen, carbon–carbon (between the carbonyl carbons), and metal–oxygen bond length comparisons to those of other complexes with similar oxidation states and to free ligand interatomic distances. A review of carbon–oxygen and carbon–carbon bond lengths shows catecholates to have C–O and C–C bond lengths of 1.35 (1) and 1.40 Å, respectively, while *o*-semiquinones exhibit C–O and C–C distances of 1.29 (1) and 1.44 Å.[6] Neither form, catecholate or *o*-semiquinone, varies much from these benchmark values. Pertinent to the work to be reported here are the distances and assignments given in Table I. The only crystallographically characterized compound containing an unreduced *o*-benzoquinone ligand (9,10-phenanthrenequinone), $MoO_2Cl_2(O_2C_{14}H_8)$, has values of 1.234 (4) and 1.530 (4) Å for C–O and C–C distances,[9] respectively.

A simple and often reliable means of evaluating the nature of a coordinated *o*-quinone is by infrared spectroscopy. Values of ν_{C-O} shift to lower energy upon coordination. Shifts of ca. 50 cm^{-1} are typical of unreduced ligands while shifts in the range 200–300 cm^{-1} are indicative of the fully reduced forms of the ligands, CAT-2.[10] The shifts in ν_{C-O} values for *o*-semiquinone ligands,

(1) Part 14: Chisholm, M. H.; Folting, K.; Huffman, J. C.; Kober, E. M. *Inorg. Chem.* **1985**, *24*, 241.

(2) Examples of "simple" oxidative additions of *o*-quinones to metals with d^n configurations are as follows. (I) For d^{10}: (a) Valentine, D., Jr.; Valentine, J. S. *J. Am. Chem. Soc.* **1970**, *92*, 5795. (b) Balch, A. L.; Sohn, J. S. *J. Am. Chem. Soc.* **1971**, *93*, 1290. (c) Cenini, S.; LaMonica, G.; Ugo, R. *J. Chem. Soc. A* **1971**, 416. (d) Cenini, S.; LaMonica, G; Navazio, G.; Sandrini, P. *J. Organomet. Chem.* **1971**, *31*, 89. (e) Barlex, D. M.; Kemmitt, R. D. W.; Littlecott, G. W. *J. Organomet. Chem.* **1974**, *65*, 253. (f) Balch, A. L. *J. Am. Chem. Soc.* **1973**, *95*, 2723. (g) Balch, A. L.; Girgis, A. Y.; Sohn, Y. S. *Inorg. Chem.* **1975**, *14*, 2327. (II) For d^8, see ref 2a,b,g and: (h) Balch, A. L.; Sohn, Y. S. *J. Organomet. Chem.* **1971**, *30*, C31. (i) Balch, A. L.; Sohn, Y. A. *J. Am. Chem. Soc.* **1972**, *94*, 1144. (j) Blake, D. M.; Bulls, R.; Mondal, J. U. *Inorg. Chem.* **1982**, *21*, 1668. (III) For d^6, see ref 2h. (IV) For d^4, see: (k) Rouschais, G.; Wilkinson, G. *J. Chem. Soc. A* **1967**, 993. (V) For d^2, see: (l) Fachinetti, C.; Floriani, G. *J. Chem. Soc., Chem. Commun.* **1972**, 790.

(3) (a) Martell, A. E.; Kahn, M. M. T. In *Inorganic Biochemistry*; Eicovn, G. L., Ed.; Elsevier: Amsterdam, 1973. (b) Thompson, R. H. *Naturally Occurring Quinones*, 2nd ed.; Academic: New York, 1971. (c) O'Connor, C. M., Wolstenholme, G. E. W., Eds. *Quinones in Electron Transport*; Little, Brown: Boston, 1960.

(4) (a) Spence, J. T.; Kronek, P. *J. Less-Common Met.* **1974**, *36*, 465. (b) Patai, S., Ed. *The Chemistry of Quinonoid Compounds*; Wiley: New York, 1974; Parts 1 and 2. (c) Carrano, C. J.; Raymond, K. N. *Acc. Chem. Res.* **1979**, *12*, 183.

(5) (a) McCleverty, J. A. *Prog. Inorg. Chem.* **1968**, *10*, 49. (b) Schrauzer, G. N. *Acc. Chem. Res.* **1969**, *2*, 72. (c) Eisenberg, R. *Prog. Inorg. Chem.* **1970**, *12*, 295.

(6) Buchanan, R. M.; Pierpont, C. G. *Coord. Chem. Rev.* **1981**, *38*, 45.

(7) Chambers, J. In *Chemistry of Quinonoid Compounds*; Patai, S., Ed.; Wiley: New York, 1974; Part 1.

(8) Some examples are: (a) Cooper, S. R.; Raymond, K. N.; Sofen, S. R.; Wave, D. C. *Inorg. Chem.* **1979**, *18*, 234. (b) Buchanan, R. M.; Downs, H. H.; Pierpont, C. G. *Inorg. Chem.* **1979**, *18*, 1736. (c) Buchanan, R. M.; Claflin, J.; Pierpont, C. G. *Inorg. Chem.* **1983**, *22*, 2552. For a theoretical study of *o*-quinone complexes of chrominum and vanadium, which exhibit multistep redox processes, see: (d) Fenske, R. F.; Gordon, D. J. *Inorg. Chem.* **1982**, *21*, 2907.

(9) Down, H. H.; Pierpont, C. G. *Inorg. Chem.* **1977**, *16*, 2970.

(10) This observation has been noted before: (a) Downs, H. H.; Pierpont, C. G. *Inorg. Chem.* **1975**, *14*, 343. (b) Reference 2c,g. (c) Calderazzo, F.; Floriani, C.; Henzi, R. *J. Chem. Soc., Dalton Trans.* **1972**, 2640.

0020-1669/88/1327-2059$01.50/0

Table I. Pertinent Bond Distances (Å) for *o*-Quinone Derivatives of Molybdenum Showing the Assignment of Charge for the Ligands in Their Reduced Forms CAT-2 and SQ-1 Shown by **1** and **2**, Respectively, in the Text

complex	Mo–O	C–O	C–C	ref
$MoO_2(Cat)_2^{2-}$	2.05, 2,17	*a*	*a*	*b*
$Mo_2O_5(Cat)_2^{2-}$	2.07, 2.37	1.36	1.39	*c*
$Mo_2O_5(3,5\text{-}DBCat)_2^{2-}$	2.157 (5), 2.392 (5)	1.37 (2)	1.37 (2)	*d*
$Mo_2O_2(3,5\text{-}DBCat)_4$	1.965 (3), 2.325 (3)	1.360 (6)	1.396 (6)	*e*
$Mo_2(O\text{-}Cl_4Cat)_6$	1.919 (6)	1.34 (1)	1.39 (1)	*f*
$Mo(9,20\text{-}phenCat)_2(9,10\text{-}phenSQ)^i$	1.952 (5)	1.346 (9)	1.348 (10)	*g*
$Mo(9,10\text{-}phenCat)_2(9,10\text{-}phenSQ)^j$	1.978 (5)	1.312 (8)	1.427 (10)	*f*
$Mo_2O_5(9,10\text{-}phenSQ)_2$	2.141 (4), 2.495 (4)	1.312 (7)	1.426 (9)	*h*

[a] Not reported. [b] Tkachev, V. V.; Atovmyan, L. O. *Coord. Chem. (Engl. Transl.)* **1975**, *1*, 845. [c] Atovmyan, L. O.; Tkachev, V. V.; Shishova, T. G. *Dokl. Akad. Nauk SSSR* **1972**, *205*, 609. [d] Wilshire, J. P.; Leon, L.; Bosserman, P.; Sawyer, D. T.; Buchanan, R. M.; Pierpont, C. G. *Chem. Uses Molybdenum, Proc. Int. Conf.* **1979**, *3*, 264. [e] Buchanan, R. M.; Pierpont, C. G. *Inorg. Chem.* **1979**, *18*, 1616. [f] Pierpont, C. G.; Downs, H. H. *J. Am. Chem. Soc.* **1975**, *97*, 2123. [g] Pierpont, C. G.; Buchanan, R. M. *J. Am. Chem. Soc.* **1975**, *97*, 4912. [h] Pierpont, C. G.; Buchanan, R. M. *J. Am. Chem. Soc.* **1975**, *97*, 6450. [i] Distances are given for the assigned CAT-2 ligand. [j] Distances are given for the assigned SQ-1 ligand.

SQ-1, span the range 50–200 cm^{-1}, which means that the identification of a *o*-semiquinone ligand based on the shift of the value of ν_{C-O} is not always possible.

Compounds containing metal-to-metal multiple bonds contain a reservoir of electrons for oxidative processes. It has been shown that $M_2(OR)_6$ compounds[11] with M–M bond configuration $\sigma^2\pi^4$ will react via successive oxidative additions resulting in M≡M- and M—M-containing compounds (eq 2) exhibiting $\sigma^2\pi^2$ and σ^2 M–M bonding configurations, respectively.[12,13]

$$\underset{M\equiv M}{M_2(OR)_6} \xrightarrow{X_2} \underset{M=M}{M_2(OR)_6X_2} \xrightarrow{X_2} \underset{M-M}{M_2(OR)_6X_4} \qquad (2)$$

It should be noted, however, that these oxidative processes are not well-understood in a mechanistic sense, nor do the limited known examples provide proof of generality or reliability. In fact it is rarely possible to predict when in an oxidative process oxidation will stop.

In light of the rich redox chemistry of *o*-benzoquinones and the present knowledge of coordination chemistry surrounding the $M_2^{6+}(M\equiv M)$ unit (M = Mo, W),[14] one of two possibilities can be envisaged as resulting from reactions of $M_2(OR)_6$ compounds with various *o*-benzoquinones: (1) simple adduct formation as a Lewis base to form another of the ubiquitous $M_2(OR)_6(L\frown L)/M_2(OR)_6L_2$ compounds,[11b,14h] or (2) redox processes to form $M_2(OR)_6(L\frown L^-)_y/M_2(OR)_6(L\frown L^{2-})_y$ compounds.

Redox properties of the *o*-benzoquinones are, in principle, tunable by substituent effects on the ring[15] as are those of the M≡M triple bonds as a function of alkoxide R groups and the metal. Thus, the potential reactions between *o*-benzoquinones and $M_2(OR)_6$ compounds appeared quite intriguing and certainly well worthy of investigation. We report here on our findings.

Experimental Section

Physical Techniques. ^1H NMR spectra were recorded on a Nicolet NT-360 360-MHz spectrometer or a Varian Associates HR-220 220-MHz spectrometer in dry and oxygen-free toluene-d_8, benzene-d_6, or dichloromethane-d_2. ^1H NMR chemical shifts are reported relative to the CHD_2 quintet of toluene-d_8 (δ 2.09), the ^1H impurity of benzene-d_6 (δ 7.15), or the triplet of $CHDCl_2$ (δ 5.32).

Infrared spectra were recorded on a Perkin-Elmer 283 spectrophotometer as Nujol mulls between CsI plates. Electronic absorption spectra were obtained with a Perkin-Elmer 330 spectrophotometer. Samples were run versus a solvent blank by using matched 1.00-cm or 1.0-mm quartz cells.

Cyclic voltammograms were obtained with a PAR 173 potentiostat, a PAR 175 programmer, and a Houston 2000 XY recorder. A single-compartment cell was used with a platinum-bead or -gauze working electrode, a platinum-wire auxiliary electrode, and a 0.01 M $AgNO_3$-(CH_3CN)/Ag-wire pseudo reference electrode. A 0.2 M solution of tetra-*n*-butylammonium hexafluorophosphate (TBAH) was employed as a supporting electrolyte. Internal resistance (IR) compensation was not employed. Ferrocene was used as a calibrant ($E_{1/2}$ = +0.08 V) before each run. The peak splitting for this couple (without IR compensation) was consistent with a reversible couple (60–65 mV).

Syntheses. All reactions were carried out under an atmosphere of dry and oxygen-free nitrogen by utilizing Schlenk and glovebox techniques. Hexane and toluene were degassed and eluted from an activated copper catalyst and molecular sieve columns and subsequently stored under nitrogen. Pyridine was distilled from KOH and stored as above. Sodium–benzophenone ketyl was used to purify THF, which likewise was distilled onto sieves and stored under nitrogen.

The starting materials, $M_2(OR)_6$,[11] were synthesized as previously described. The *o*-benzoquinones, 9,10-phenanthrenequinone and tetrachloro-1,2-benzoquinone, were purchased from Aldrich and used without purification. Elemental analyses were performed by Alfred Bernhardt Microanalitisches Laboratorium, Elbach, West Germany, and Canadian Microanalytical Services Ltd., Vancouver, British Columbia, Canada.

$Mo_2(OR)_6 + 2O_2C_6Cl_4$ (R = *i*-Pr, *neo*-Pe). The standard preparative method used is illustrated by the following reaction involving $Mo_2(O\text{-}i\text{-}Pr)_6$. $Mo_2(O\text{-}i\text{-}Pr)_6$ (800 mg, 1.47 mmol) was dissolved in toluene (15 mL) in a 50-mL round-bottomed Schlenk flask. A 25-mL pressure-equalized dropping funnel containing tetrachloro-1,2-benzoquinone (725 mg, 2.94 mmol) in methylene chloride (20 mL) was fitted to the Schlenk flask. Tetrachloro-1,2-benzoquinone was added over 6 h at 0 °C with stirring. During this time the solution changed from yellow to violet-black. The reaction mixture was stirred 8 h, followed by crystallization at room temperature over 24 h, providing black crystals of $Mo_2(OR)_6(O_2C_6Cl_4)_2$ in 45% yield. The crystals were filtered from the mother liquor and dried in vacuo. Yields may be increased to ca. 70% by reducing the volume of the filtrate with subsequent recrystallization at −40 °C, although the quality of the crystals is poorer.

$Mo_2(O\text{-}i\text{-}Pr)_6(O_2C_6Cl_4)_2$ (1). IR: 1540 w, 1410 s, 1320 w, 1275 w, 1250 m, 1160 m, 1125 (shoulder), 1100 s, 1000 m, 990 m, 975 s, 957 s, 935 s, 850 m, 812 s, 787 m, 615 w, 600 s, 570 w, 510 w cm^{-1}. ^1H NMR (toluene-d_8, 220 MHz): t-OCHMe_2, δ 0.67 (doublet, 6 Hz, 24 H); μ-OCHMe_2, δ 1.63 (doublet, 6 Hz, 12 H); t-OCHMe$_2$, δ 4.40 (septet, 6 Hz, 4 H); μ-OCHMe$_2$, δ 6.19 (septet, 6 Hz, 2 H). Anal. Found (calcd): C, 34.64 (34.69); H, 4.12 (4.05); Cl, 27.90 (28.25). UV–vis (hexane): λ_{max} 605, 422, 333, 291 nm, with shoulders (indicative of phenyl ring).

$Mo_2(O\text{-}neo\text{-}Pe)_6(O_2C_6Cl_4)_2$ (2). IR: 1540 w, 1373 m, 1363 m, 1340 w, 1270 w, 1260 m, 1227 w, 1130 (shoulder), 1120 (shoulder), 1000 s (broad), 980 s, 930 w, 817 s, 785 s, 680 w, 610 (shoulder), 600 s, 570 w, 510 w cm^{-1}. ^1H NMR (toluene-d_8, 360 MHz): t-OCH$_2$CMe_3, δ 0.88 (singlet, 36 H); μ-OCH$_2$CMe_3, δ 1.00 (singlet, 18 H); t-OCH_2CMe$_3$, δ 3.23 (singlet, 8 H); μ-OCH_2CMe$_3$, δ 5.11 (singlet, 4 H). UV–vis (hexane): λ_{max} 595, 436, 290 nm.

(11) (a) M = Mo: Chisholm, M. H.; Cotton, F. A.; Murillo, C. A.; Reichert, W. W. *Inorg. Chem.* **1977**, *16*, 1801. (b) M = W: Akiyama, M.; Chisholm, M. H.; Cotton, F. A.; Extine, M. W.; Haitko, D. A.; Little, D.; Fanwick, P. E. *Inorg. Chem.* **1979**, *18*, 2311.

(12) (a) Chisholm, M. H.; Kirkpatrick, C. C.; Huffman, J. C. *Inorg. Chem.* **1981**, *20*, 871. (b) Chisholm, M. H.; Ratermann, A. L.; Huffman, J. C. *Inorg. Chem.* **1983**, *22*, 4100. (c) Chisholm, M. H.; Ratermann, A. L.; Smith, C. A.; Huffman, J. C. *Inorg. Chem.* **1984**, *23*, 1596.

(13) For information regarding this qualitative bonding picture in M–M multiply bonded compounds, see: (a) Cotton, F. A. *Chem. Soc. Rev.* **1975**, *4*, 27. (b) Mortola, A. P.; Moskowitz, J. W.; Rosch, M. *Int. J. Quantum Chem.* **1974**, *58*, 161. (c) Kolari, H. J.; Norman, J. G. *J. Am. Chem. Soc.* **1975**, *97*, 33. (d) Cotton, F. A. *J. Less-Common Met.* **1977**, *54*, 3.

(14) (a) Chisholm, M. H. *Transition Met. Chem. (Weinheim, Ger.)* **1978**, *3*, 321. (b) Chisholm, M. H.; Cotton, F. A. *Acc. Chem. Res.* **1978**, *11*, 356. (c) *Adv. Chem. Ser.* **1979**, *No. 173*, 396. (d) Chisholm, M. H. *ACS Symp. Ser.* **1981**, *No. 155*, 17. (e) Chisholm, M. H.; Rothwell, I. P. *Prog. Inorg. Chem.* **1982**, *29*, 1. (f) Chisholm, M. H. *J. Organomet. Chem.* **1982**, *239*, 79. (g) Chisholm, M. H. *ACS Symp. Ser.* **1983**, *No. 211*, 243. (h) Chisholm, M. H. *Polyhedron* **1983**, *2*, 681. (i) Chisholm, M. H. *Angew. Chem., Int. Ed. Engl.* **1986**, *25*, 21.

(15) Morrison, M. M.; Sawyer, D. T.; Stallings, M. D. *Inorg. Chem.* **1981**, *20*, 2655.

$Mo_2(O\text{-}i\text{-}Pr)_8$ + 2$O_2C_6Cl_4$. $Mo_2(O\text{-}i\text{-}Pr)_8$ was synthesized as previously described.[16] $Mo_2(O\text{-}i\text{-}Pr)_8$ (500 mg, 0.753 mmol) was dissolved in toluene (10 mL) in a 50-mL round-bottomed Schlenk flask. Tetrachloro-1,2-benzoquinone (370 mg, 1.50 mmol) was added as a methylene chloride solution (15 mL) via a pressure-equalized dropping funnel at 0 °C over 6 h. The originally midnight blue solution turned a dark violet-black as the reaction proceeded. The reaction was allowed to come to room temperature over 10 h, and the solvent was subsequently removed in vacuo. The ^1H NMR spectrum of the violet-black product showed $Mo_2(O\text{-}i\text{-}Pr)_6(O_2C_6Cl_4)_2$ (**1**) as the only product. A small-scale reaction involving $Mo_2(O\text{-}i\text{-}Pr)_8$ (50 mg, 0.075 mmol) and tetrachloro-1,2-benzoquinone (37 mg, 0.15 mmol) dissolved in toluene-d_8 (1.5 mL) was undertaken in a 25-mL round-bottomed flask equipped with a gastight Teflon Kontes valve to determine the identity of the side products of the reaction. The volatile components were vacuum-transferred into a NMR tube. 2-Propanol and acetone were identified by ^1H NMR spectroscopy. The addition of authentic samples of acetone and 2-propanol to the NMR tube yielded only increased signal intensities; no new signals were observed. ^1H NMR (toluene-d_8, 220 MHz); acetone, δ 1.59 (singlet);[17] 2-propanol, δ 0.96 (doublet, 6 Hz), 3.70 (septet, 6 Hz).

$Mo_2(OR)_6$ + 2 9,10-Phenanthrenequinone (R = *i*-Pr, *neo*-Pe). The standard preparation of these compounds is illustrated as follows. $Mo_2(O\text{-}i\text{-}Pr)_6$ (600 mg, 1.10 mmol) was placed in a 50-mL round-bottomed Schlenk flask and dissolved in methylene chloride (15 mL). 9,10-Phenanthrenequinone (458 mg, 2.20 mmol) was added dropwise as a methylene chloride solution (15 mL) at 0 °C over 8 h via a pressure-equalized dropping funnel. After complete addition of 9,10-phenanthrenequinone the resulting solution was stirred 8 h at room temperature. The volume of the reaction mixture was reduced to ca. 5–10 mL, and the flask was placed in the freezer at −30 °C. The resultant black crystals were filtered and dried in vacuo, furnishing a 30% yield. Continued removal of solvent with subsequent crystallization may increase the yield; however, after 60% yield other products begin to cocrystallize, i.e. $Mo_2(OR)_4(O_2C_{14}H_8)_3$ and $Mo_2(OR)_2(O_2C_{14}H_8)_4$ (vide infra).

$Mo_2(O\text{-}i\text{-}Pr)_6(O_2C_{14}H_8)_2$ (3). IR: 1600 w, 1563 w, 1492 w/m, 1333 w/m, 1258 w, 1221 w, 1160 m, 1100 s, 1054 m, 1030 m, 993 m, 957 s, 850 m, 788 m, 753 s, 720 s, 685 m, 600 s (broad), 465 w, 400 w cm^{-1}. ^1H NMR (methylene-d_2 chloride, 360 MHz, 21 °C): t-OCHMe_2, δ 0.90 (doublet, 6 Hz, 24 H); μ-OCHMe_2, δ 1.95 (doublet, 6 Hz, 12 H); t-OCHMe$_2$, δ 4.67 (septet, 6 Hz, 4 H); μ-OCHMe$_2$, δ 6.40 (doublet, 6 Hz, 2 H); 9,10-phenanthrenequinone, δ 7.51 (triplet, 7.2 Hz, 4 H), 7.66 (triplet, 7.2 Hz, 4 H), 8.26 (doublet, 8.2 Hz, 4 H), 8.68 (doublet, 8.2 Hz, 4 H). Anal. Found (calcd): C, 56.66 (57.38); H, 6.01 (6.03). UV–vis (hexane): λ_{max} 752, 424 (shoulder), 380 (shoulder), 357, 289 (shoulder), 284 (shoulder), 280, 275 (shoulder), 271 nm (shoulder).

$Mo_2(O\text{-}neo\text{-}Pe)_6(O_2C_{14}H_8)_2$ (4). IR: 1603 w, 1570 w, 1496 m, 1328 w, 1288 w, 1260 m, 1200 w, 1157 w, 1110 m, 1050 s (broad), 937 w, 790 m, 754 s, 725 s, 680 s, 600 m, 550 w/m, 525 m/s, 480 w, 460 w, 405 m cm^{-1}. ^1H NMR (toluene-d_8, 360 MHz, 21 °C): t-OCH$_2$CMe_3, δ 1.03 (singlet, 36 H); μ-OCH$_2$CMe_3, δ 1.36 (singlet, 18 H); t-OCH_2CMe$_3$, δ 4.75 (broad singlet, 8 H); μ-OCH_2CMe$_3$, δ 5.05 (broad singlet, 4 H); 9,10-phenanthrenequinone, δ 7.07 (triplet, 7.2 Hz, 4 H), 7.37 (triplet, 7.2 Hz, 4 H), 7.94 (doublet, 8.2 Hz, 4 H), 8.20 (doublet, 8.2 Hz, 4 H).

$Mo_2(OR)_6$ + 4$O_2C_6Cl_4$ (R = *i*-Pr, *neo*-Pe). The following depicts the standard method of preparation of these two compounds. $Mo_2(O\text{-}i\text{-}Pr)_6$ (554 mg, 1.01 mmol) was dissolved in methylene chloride (10 mL). A methylene chloride solution (20 mL) of tetrachloro-1,2-benzoquinone (497 mg, 2.02 mmol) was added over 3 h at room temperature by using a pressure-equalized dropping funnel. The solution changed from yellow to violet-black. After the reaction mixture was stirred for 8 h, its volume was reduced to 10 mL. Dark crystals formed over a 24-h period at room temperature and were subsequently separated by filtration from the mother liquor to give $Mo_2(O\text{-}i\text{-}Pr)_2(O_2C_6Cl_4)_4$ in 90% recrystallized yield.

A small-scale reaction was undertaken to determine the fate of the alkoxide groups. $Mo_2(O\text{-}i\text{-}Pr)_6$ (50 mg, 0.090 mmol) and tetrachloro-1,2-benzoquinone (88 mg, 0.36 mmol) were placed in a 25-mL round-bottomed flask fitted with a gastight Kontes valve into which benzene-d_6 (ca. 1 mL) was vacuum-transferred. The reaction mixture was stirred for 8 h, after which the volatile components and benzene-d_6 were transferred to a NMR tube by vacuum techniques. The volatile components were identified as acetone and 2-propanol by ^1H NMR spectroscopy and comparison with authentic samples.

$Mo_2(O\text{-}i\text{-}Pr)_2(O_2C_6Cl_4)_4$ (5). IR: 1540 w, 1408 w, 1320 w, 1274 w, 1260 m, 1228 w, 1165 w, 1130 w, 1092 (shoulder), 1090 m, 1000 m, 937 s, 918 s, 860 s, 816 m, 785 m/s, 636 m, 611 (shoulder), 601 m, 587 m, 571 w, 513 w, 473 w cm^{-1}. ^1H NMR (methylene-d_2 chloride, 360 MHz, 21 °C): μ-OCHMe_2, δ 1.19 (doublet, 6 Hz, 12 H); μ-OCHMe$_2$, δ 5.72 (septet, 6 Hz, 2 H). ^1H NMR (methylene-d_2 chloride, 360 MHz, −65 °C): μ-OCHMe_2, δ 1.16 (overlapping doublets, 6 Hz, 12 H); μ-OCHMe$_2$, δ 5.72 (septet, 6 Hz, 2 H). Anal. Found (calcd): C, 29.32 (27.84); H, 1.59 (1.08); Cl, 42.04 (43.86).

$Mo_2(O\text{-}neo\text{-}Pe)_2(O_2C_6Cl_4)_4$ (6). ^1H NMR (methylene-d_2 chloride, 360 MHz, 21 °C): μ-OCH$_2$CMe_3, δ 0.86 (singlet, 18 H); μ-OCH_2CMe$_3$, δ 4.95 (broad singlet, 4 H). ^1H NMR (methylene-d_2 chloride, 360 MHz, −50 °C): μ-OCH$_2$CMe_3, δ 0.86 (singlet, 18 H); μ-OCH_2CMe$_3$, δ 4.95 (AB quartet, 4 H).

$Mo_2(OR)_6$ + 4 9,10-Phenanthrenequinone (R = *i*-Pr, *neo*-Pe). A representative synthesis for the stated reactions is given. $Mo_2(O\text{-}i\text{-}Pr)_6$ (600 mg, 1.10 mmol) was dissolved in methylene chloride (10 mL) in a 50-mL pear-shaped Schlenk flask. A solution of 9,10-phenanthrenequinone (915 mg, 4.40 mmol) in methylene chloride (20 mL) was added dropwise to the yellow solution of $Mo_2(O\text{-}i\text{-}Pr)_6$ via a pressure-equalized dropping funnel over a period of 3 h at room temperature. Upon completion of the addition of the 9,10-phenanthrenequinone solution the resulting reaction mixture was stirred 6 h and subsequently placed in the freezer at −30 °C. Violet-black crystals of $Mo_2(O\text{-}i\text{-}Pr)_2(O_2C_{14}H_8)_4$ appeared after 2 days. The crystals were filtered and dried in vacuo; yield 45%. Further reduction of solvent volume and crystallization raised the yield to 70%.

The fate of the alkoxide groups was determined by reacting $Mo_2(O\text{-}i\text{-}Pr)_6$ (50 mg, 0.090 mmol) and 9,10-phenanthrenequinone in a 25-mL reaction bulb outfitted with a gastight Kontes valve in benzene-d_6. The reaction mixture was stirred for 8 h, at which time the volatile components and benzene-d_6 were vacuum-transferred to a NMR tube. 2-Propanol and acetone were identified upon comparison to authentic samples.

$Mo_2(O\text{-}i\text{-}Pr)_2(O_2C_{14}H_8)_4$ (7). IR: 1600 w, 1560 m, 1508 w, 1492 m, 1420 m, 1415 (shoulder), 1360 m, 1310 m, 1280 w, 1242 w, 1230 w, 1180 w, 1155 w, 1112 w, 1094 s, 1030 w, 950 s (broad), 855 m (doublet), 760 w, 745 s, 750 s, 605 s, 510 s cm^{-1}. ^1H NMR (methylene-d_2 chloride, 360 MHz, 21 °C): μ-OCHMe_2, δ 1.58 (doublet, 6 Hz, 12 H); μ-OCHMe$_2$, δ 5.85 (septet, 6 Hz, 2 H); 9,10-phenanthrenequinone, δ 7.46 (triplet, 7.2 Hz), 7.60 (broad), 7.92 (broad), 8.58 (doublet, 8.3 Hz). ^1H NMR (methylene-d_2 chloride, 360 MHz, −65 °C): μ-OCHMe_2, δ 1.53 (overlapping doublets, 6 Hz, 12 H); μ-OCHMe$_2$, δ 5.85 (septet, 6 Hz, 2 H); 9,10-phenanthrenequinone, δ 7.43 (triplet, 7.2 Hz, 1 H), 7.49 (overlapping triplets, 7.2 Hz, 2 H), 7.70 (triplet, 7.2 Hz, 1 H), 7.71 (doublet, 8.2 Hz, 1 H), 8.04 (doublet, 8.2 Hz, 1 H), 8.04 (doublet, 8.2 Hz, 1 H), 8.56 (doublet, 8.2 Hz, 1 H), 8.59 (doublet, 8.2 Hz, 1 H). Anal. Found (calcd): C, 63.89 (65.15); H, 4.63 (4.03).

$Mo_2(O\text{-}neo\text{-}Pe)_2(O_2C_{14}H_8)_4$ (8). ^1H NMR (methylene-d_2 chloride, 360 MHz, 21 °C): μ-OCH$_2$CMe_3, δ 1.04 (singlet, 18 H); μ-OCH_2CMe$_3$, δ 4.99 (broad singlet, 4 H); 9,10-phenanthrenequinone, δ 7.47 (triplet, 7.2 Hz, 2 H), 7.61 (broad), 7.88 (broad), 8.59 (doublet, 8.2 Hz, 2 H).

$Mo_2(O\text{-}i\text{-}Pr)_6$ + 3 9,10-Phenanthrenequinone. $Mo_2(O\text{-}i\text{-}Pr)_6$ (550 mg, 1.01 mmol) was dissolved in a mixture of methylene chloride (10 mL) and tetrahydrofuran (5 mL) in a 50-mL round-bottomed Schlenk flask. A methylene chloride solution (15 mL) of 9,10-phenanthrenequinone (578 mg, 2.78 mmol) was added dropwise over 8 h at room temperature via a pressure-equalized dropping funnel. After the reaction mixture was stirred an additional 8 h, the volume in the flask was reduced by half. The reaction vessel was then placed in the freezer at −30 °C, affording black crystals after 2 days. The solution was filtered, and the crystals were dried in vacuo. The product is predominantly $Mo_2(O\text{-}i\text{-}Pr)_6(O_2C_{14}H_8)_2$ with a lesser amount of $Mo_2(O\text{-}i\text{-}Pr)_4(O_2C_{14}H_8)_3$ as determined by ^1H NMR spectroscopy.

$Mo_2(O\text{-}i\text{-}Pr)_4(O_2C_{14}H_8)_3$ (9). ^1H NMR (methylene-d_2 chloride, 360 MHz, −55 °C): t-OCHMe_2, δ 0.51 (doublet, 6 Hz, 6 H), 1.31 (doublet, 6 Hz, 6 H); μ-OCHMe_2, δ 1.98 (overlapping doublets); t-CHMe$_2$, δ 4.61 (septet, 6 Hz, 2 H); μ-OCHMe$_2$, δ 6.79 (septet, 6 Hz, 2 H).

$W_2(O\text{-}i\text{-}Pr)_6L_2$ (L = py, HNMe$_2$) + 2 9,10-Phenanthrenequinone. $W_2(O\text{-}i\text{-}Pr)_6$ (650 mg, 0.740 mmol) was dissolved in toluene (10 mL) in a 50-mL pear-shaped Schlenk flask. A methylene chloride solution (15 mL) of 9,10-phenanthrenequinone (307 mg, 1.48 mmol) was introduced dropwise over 3 h at 0 °C via a pressure-equalized dropping funnel. After all of the 9,10-phenanthrenequinone solution was added, the reaction mixture was allowed to come to room temperature with stirring over 12 h. The flask was then placed in the freezer at −25 °C for 4 days, at which time a small amount of red-brown microcrystalline product had appeared. After filtration, complete removal of the solvent in vacuo provided a red-brown product whose ^1H NMR spectrum matched exactly that of the microcrystalline product. As judged by ^1H NMR, the product was a mixture of $W_2(O\text{-}i\text{-}Pr)_6(O_2C_{14}H_8)_2$, $W_2(O\text{-}i\text{-}Pr)_4(O_2C_{14}H_8)_3$, and $W_2(O\text{-}i\text{-}Pr)_2(O_2C_{14}H_8)_4$. Starting material was also present in the ^1H

(16) Chisholm, M. H.; Reichert, W. W.; Thornton, P. *J. Am. Chem. Soc.* **1978**, *100*, 2744.

(17) Pavia, D. L.; Lampman, G. M.; Kriz, G. S., Jr. *Introduction to Spectroscopy*; W. B. Saunders: Philadelphia, 1979; Chapter 4, p 127 ff.

Table II. Summary of Crystallographic Data[a]

	I	II	III	IV
empirical formula	$Mo_2Cl_8O_{10}C_{30}H_{42}$	$Mo_2Cl_8O_{10}C_{42}H_{60}$	$Mo_2O_{10}C_{54}H_{52}\cdot 2C_4OH_8$	$Mo_2Cl_8O_9N_4C_{32}H_{22}$
color of cryst	brown	black	dark brown or black	red
crystal dimens, mm	0.08 × 0.07 × 0.152	small, irreg split fragment	0.35 × 0.35 × 0.35 mm	0.05 × 0.05 × 0.05
space group	$P\bar{1}$	$P2_1/c$	$P\bar{1}$	$P2_1/c$
cell dimens				
temp, °C	−160	−160	−163	−162
a, Å	10.579 (5)	11.826 (7)	18.520 (10)	31.613 (15)
b, Å	11.014 (5)	14.176 (10)	13.763 (6)	13.365 (4)
c, Å	9.619 (4)	17.682 (12)	12.920 (6)	18.207 (6)
α, deg	108.38 (2)		114.69 (3)	
β, deg	108.44 (2)	96.34 (3)	110.56 (2)	96.27 (2)
γ, deg	81.49 (2)		71.97 (3)	
Z (molecules/cell)	1	2	2	8
vol, Å^3	1007.54	2943.29	2749.85	7646.76
calcd density, g/cm^3	1.711	1.353	1.446	1.880
wavelength, Å	0.710 69	0.710 69	0.710 69	0.710 69
mol wt	1006.16	2943.29	1197.09	1082.05
linear abs coeff, cm^{-1}	11.919	8.246	5.051	12.618
detector to sample dist, cm	22.5	22.5	22.5	22.5
sample to source dist, cm	23.5	23.5	23.5	23.5
av ω scan width at half-height	0.25	0.25	0.25	0.25
scan speed, deg/min	3.0	3.0	6.0	4.0
scan width (+dispersion), deg	2.0	2.0	1.8	1.2
indiv bkgd, s	4	4	8	5
aperture size, mm	3.0 × 4.0	3.0 × 4.0	3.0 × 4.0	3.0 × 4.0
2θ range, deg	6–45	6–45	6–45	5–45
total no. of reflns collected	4068	4447	7329	11 748
no. of unique intens	2646	3759	7209	10 056
no. with $F > 0.0$	2429	3316		8677
no. with $F > \sigma(F)$	2295	3107		
no. with $F > 2.33\sigma(F)$	2119	2783		
no. with $F > 3.00\sigma(F)$			6257	7297
$R(F)$	0.0481	0.1527	0.0614	0.0616
$R_w(F)$	0.0447	0.1457	0.0653	0.0507
goodness of fit for the last cycle	1.018	3.237	1.583	1.111
max Δ/σ for last cycle	0.05	0.05	0.05	0.05

[a] Legend: (I) $Mo_2(O\text{-}i\text{-}Pr)_6(O_2C_6Cl_4)_2$; (II) $Mo_2(O\text{-}neo\text{-}Pe)_6(O_2C_6Cl_4)_2$; (III) $Mo_2(O\text{-}i\text{-}Pr)_4(O_2C_{14}H_8)_3$; (IV) $[pyH]_2[(MoO_2(O_2C_6Cl_4)py)_2O]$.

NMR spectrum. Attempts to obtain any member of this series in a pure state failed.

$W_2(O\text{-}i\text{-}Pr)_6(O_2C_{14}H_8)_2$ (10). ^{1}H NMR (methylene-d_2 chloride, 220 MHz, 22 °C): t-OCHMe_2, δ 0.62 (doublet, 6 Hz, 24 H); μ-OCHMe_2, δ 2.15 (doublet, 6 Hz, 12 H); t-OCHMe$_2$, δ 5.07 (septet, 6 Hz, 4 H); μ-OCHMe$_2$, δ 6.66 (septet, 6 Hz, 2 H).

$W_2(O\text{-}i\text{-}Pr)_4(O_2C_{14}H_8)_3$ (11). ^{1}H NMR (methylene-d_2 chloride, 220 MHz, 22 °C): t-OCHMe_2, δ 1.08 (doublet, 6 Hz, 12 H); μ-OCHMe_2, δ 1.61 (doublet, 6 Hz, 12 H); t-OCHMe$_2$, δ 4.93 (septet, 6 Hz, 2 H); μ-OCHMe$_2$, δ 7.10 (septet, 6 Hz, 2 H).

$W_2(O\text{-}i\text{-}Pr)_2(O_2C_{14}H_8)_4$ (12). ^{1}H NMR (methylene-d_2 chloride, 220 MHz, 22 °C): μ-OCHMe_2, δ 1.25 (doublet, 6 Hz, 6 H); μ-OCHMe$_2$, δ 5.60 (septet, 6 Hz, 2 H).

$Mo_2(O\text{-}t\text{-}Bu)_6 + 2O_2C_6Cl_4$. $Mo_2(O\text{-}t\text{-}Bu)_6$ (575 mg, 0.910 mmol) was dissolved in a mixture of tetrahydrofuran (10 mL) and methylene chloride (10 mL) in a 50-mL round-bottomed Schlenk flask. Tetrachloro-1,2-benzoquinone (449 mg, 1.82 mmol) was added via a pressure-equalized dropping funnel as a methylene chloride solution (15 mL) over 5 h at room temperature. The initial orange of the hexaalkoxide solution quickly changed to blue as the reaction proceeded. Upon completion of the addition of the tetrachloro-1,2-benzoquinone solution the reaction mixture was stirred an additional 6 h and then allowed to stand undisturbed for 36 h. Some blue microcrystals began to form, and the flask was placed in the freezer at −25 °C for 8 h. Filtration of the reaction mixture afforded small blue platelets, **14**, of uncertain composition.

Redissolving the small blue platelets in methylene chloride (10 mL) or tetrahydrofuran (10 mL) re-formed the blue solution. Addition of pyridine (1 equiv/equiv of Mo based on $Mo_2(O\text{-}t\text{-}Bu)_6$) caused the solution to change to red. The resulting red solution was stirred 1 h and left undisturbed at room temperature for 12 h. Red crystals appeared and were collected by filtration and dried in vacuo. The ^{1}H NMR spectrum of the red crystals showed only the presence of coordinated pyridine over the temperature range of +50 to −30 °C. The red product is $[pyH]_2[(MoO_2(O_2C_6Cl_4)py)_2O]$ (**13**).

$[(MoO_2(O_2C_6Cl_4)py)_2O][pyH]_2$ (13). IR: 1770 w, 1630 w, 1600 m, 1574 w, 1520 w, 1472 w, 1260 w, 1230 s, 1211 (shoulder), 1190 m, 1120 w, 1031 m, 1022 w, 1010 w, 978 w, 955 s, 908 s, 775 m/s, 755 m, 672 w, 655 s, 593 m, 585 m cm^{-1}. ^{1}H NMR (acetone-d_6, 360 MHz, 21 °C): δ 7.50 (triplet, 6.7 Hz, 2 H), 7.92 (triplet, 7.6 Hz, 1 H), 8.69 (doublet, 2.9 Hz, 2 H). Anal. Found (calcd): C, 39.17 (35.50); H, 2.55 (2.03); Cl, 25.96 (26.22).

Blue Compound (14). IR: 1465 s, 1280 w, 1250 m, 1043 w, 987 s, 966 (shoulder), 855 w, 818 s, 790 w, 583 s, 550 (shoulder), 490 w, 410 w cm^{-1}. ^{1}H NMR (methylene-d_2 chloride, 220 MHz, 22 °C): δ 1.42 (broad), 3.58 (broad), ratio of 1:1. Anal. Found: C, 28.90; H, 2.88; Cl, 22.20. Electrochemistry: two quasi-reversible waves, 0.205/0.105 and −0.133/−0.230 V, in tetrahydrofuran (0.1 M TBAH).

Crystallographic Studies. General operating procedures and listings of programs have been given previously.[18] A summary of crystal data is given in Table II.

$Mo_2(O\text{-}i\text{-}Pr)_6(O_2C_6Cl_4)_2$. A small, irregular fragment was selected and transferred to the goniostat by using the usual inert-atmosphere techniques. The crystal was cooled to −160 °C, and all characterization and data collection were carried out at this temperature. The data were processed in the usual manner; no absorption corrections were carried out.

The structure was solved by means of direct methods and standard Fourier techniques. All hydrogen atoms were located in a difference electron density map and were included in the least-squares refinements with isotropic thermal parameters. The final difference map was essentially featureless, the largest peak being 0.7 e Å^{-3}. The molecule possesses a crystallographic center of symmetry.

$Mo_2(O\text{-}neo\text{-}Pe)_6(O_2C_6Cl_4)_2$. Several fragments were selected in the usual way and transferred to the goniostat. Unfortunately all samples examined were split crystals. The one finally used seemed to consist of two crystals, with intensities 20% and 80%. The data collected were of sufficiently good quality to solve the structure, but least-squares refinements were terminated at $R = 0.15$. Several atoms had nonpositive definite thermal parameters.

$Mo_2(O\text{-}i\text{-}Pr)_4(O_2C_{14}H_8)_3\cdot 2THF$. A suitable small sample was selected and transferred to the goniostat, where it was cooled to −163 °C. The crystal was characterized in the usual manner, no symmetry or extinctions were observed, and the crystal was assigned to the space group $P\bar{1}$.

(18) Chisholm, M. H.; Folting, K.; Huffman, J. C.; Kirkpatrick, C. C. *Inorg. Chem.* **1984**, *23*, 1021.

The first crystal selected and used for identification proved to be too small for data collection; hardly any diffraction maxima were observed beyond $2\theta = 25°$. A larger crystal was selected and used for data collection. This crystal was shaped like a bisphenoid with dimensions less than 0.5 mm. However, the crystal was not measured for use in absorption correction due to poorly identifiable faces.

The data collection was carried out at −163 °C by using a scan speed of 6° min^{-1} and background times of 8 s at either end of the scan width of 1.8° plus dispersion. Data were collected in the range $6 < 2\theta < 45°$; a total of 7329 reflections were measured and reduced to a unique set of 7209 reflections. No absorption correction was performed as mentioned above.

The structure was solved by locating the Mo atoms by direct methods and proceeding using the usual heavy-atom Fourier technique. The structure contains two molecules of solvent, tetrahydrofuran. One of the solvent molecules is disordered, and both molecules have quite large thermal parameters. All non-hydrogen atoms were refined by using anisotropic thermal parameters. The hydrogen atoms were not located but were inserted in calculated positions. The least-squares refinement converged at $R(F) = 0.061$.

The final difference map contained several peaks greater than 1.0 e $Å^{-3}$. Table 6 in the structure report (see supplementary material) contains a listing of the largest peaks as well as the distances and angles involving these peaks. As can be seen, most of them are in the vicinity of the disordered solvent molecules, indicating that the disorder may be more severe than we have assumed. The solvent molecules have been omitted from all of the ORTEP drawings.

$[pyH]_2[(MoO_2(O_2C_6Cl_4)py)_2O]$. A small equidimensional crystal was selected and transferred to the goniostat by using standard inert-atmosphere handling techniques. The crystal was cooled to −162 °C. A systematic search of a limited hemisphere of reciprocal space yielded a set of reflections that possessed monoclinic symmetry and exhibited systematic extinctions consistent with the space group $P2_1/c$.

The data were collected by using a quite narrow scan width due to the large cell dimension in the *a* direction. A total of 11 748 reflections were collected; after reduction and averaging a unique set of 10 056 reflections were obtained, 8677 of which were nonzero and were used in the determination of the structure. The structure was solved by locating the heavy atoms by direct methods and proceeding by usual Fourier methods. Due to the large number of atoms in the asymmetric unit and due to program limitations, no attempts were made at locating or including hydrogen atoms. The Mo and Cl atoms were refined by using anisotropic thermal parameters, while all other atoms were refined by using isotropic thermal parameters. Each molecule is associated with two molecules of pyridine hydrogen-bonded to oxygen atoms in the catechol ligand. The refinements were carried out by using 7297 reflections having *F* greater than $3\sigma(F)$.

Results and Discussion

Syntheses and Spectroscopic Studies. In hydrocarbon solvents $M_2(OR)_6$ compounds, where R = *i*-Pr and *neo*-Pe (*neo*-Pe = neopentyl), react with *o*-quinones (O⌒O) by the initial formation of the 1:2 adducts $M_2(OR)_6(O⌒O)_2$. The latter react further with *o*-quinones, yielding $M_2(OR)_4(O⌒O)_3$ and $M_2(OR)_2(O⌒O)_4$ compounds. The specific course of the reaction is dependent on the nature of the alkoxy group, the metal, and the quinone, and sometimes only a mixture of products is obtained. The specific details of the reactions and their products are given below.

$Mo_2(OR)_6$ + 2 O⌒O (R = *neo*-Pe, *i*-Pr; O⌒O = $O_2C_6Cl_4$, 9,10-Phenanthrenequinone). Yellow solutions of $Mo_2(OR)_6$ in toluene or methylene chloride change to blue-black upon addition of 2 equiv of the appropriate *o*-benzoquinone (eq 3).

$$Mo_2(OR)_6 + 2O⌒O \rightarrow Mo_2(OR)_6(O⌒O)_2 \qquad (3)$$

For reactions involving $Mo_2(O\text{-}i\text{-}Pr)_6$ the blue-black crystalline bis(catecholate)-containing product can be obtained pure in high yield by slow addition of the *o*-benzoquinone as a methylene chloride solution. When the *o*-benzoquinone is added slowly, other products, namely $Mo_2(O\text{-}i\text{-}Pr)_4(O⌒O)_3$ and $Mo_2(O\text{-}i\text{-}Pr)_2(O⌒O)_4$, are not observed by ^1H NMR in significant quantities. However, for $Mo_2(O\text{-}neo\text{-}Pe)_6$ there are always significant amounts of $Mo_2(O\text{-}neo\text{-}Pe)_4(O⌒O)_3$ and $Mo_2(O\text{-}neo\text{-}Pe)_2(O⌒O)_4$ detected by ^1H NMR in the crystallized product, making characterization of the bis(catecholate) product difficult, especially for the 9,10-phenanthrenequinone reactions. The reaction of $Mo_2(O\text{-}neo\text{-}Pe)_6$ and 2 equiv of tetrachloro-1,2-benzoquinone provides the fully reduced bis(*o*-benzoquinone) product in favorable enough yield relative to those of the other products to allow characterization by ^1H NMR and isolation of pure crystals suitable for an X-ray structural analysis.

The ^1H NMR spectra of both $Mo_2(O\text{-}i\text{-}Pr)_6(O_2C_6Cl_4)_2$ and $Mo_2(O\text{-}i\text{-}Pr)_6(O_2C_{14}H_8)_2$ in methylene-d_2 chloride are simple and nonfluxional at the probe temperature, 22 °C. Both ^1H NMR spectra are indicative of two types of O-*i*-Pr ligands of integral ratio 2:1. The spectra are consistent with the maintenance of the solid-state structure **1** in solution with the two types of alkoxides being assigned to terminal and bridging O-*i*-Pr ligands both lying on planes of molecular symmetry.

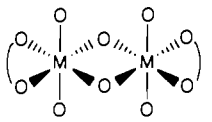

1

Also consistent with the solid-state structure are the infrared spectra of these $Mo_2(O\text{-}i\text{-}Pr)_6(O⌒O)_2$ compounds. The presence of terminal and bridging alkoxides is indicated by $\nu_{M\text{-}O}$ for $Mo_2(O\text{-}i\text{-}Pr)_6(O_2C_6Cl_4)_2$ and $Mo_2(O\text{-}i\text{-}Pr)_6(O_2C_{14}H_3)_2$ at 600, 575 cm^{-1} and at 615, 600 cm^{-1}, respectively.[19] The infrared spectra are also diagnostic of the mode of coordination of the *o*-benzoquinone. The shift to lower energy of $\nu_{C\text{-}O}$ by 200 cm^{-1} and the appearance of absorbances attributable to aromatic ring stretches are indicative of catecholate coordination (fully reduced *o*-benzoquinone). This agrees with the formulation of these compounds as d^1–d^1 M–M singly bonded compounds.

The $Mo_2(O\text{-}neo\text{-}Pe)_6(O⌒O)_2$ compounds are less well characterized owing to their contamination with other products. The ^1H NMR data and infrared data for $Mo_2(O\text{-}neo\text{-}Pe)_6(O_2C_6Cl_4)_2$ are consistent with the solid-state structure and support the view of this compound as a M–M singly bonded, d^1–d^1 dimer with terminal and bridging alkoxides in the ratio 2:1 and with terminal equatorial catecholate ligands. However, $Mo_2(O\text{-}neo\text{-}Pe)_6(O_2C_{14}H_8)_2$ cannot be efficiently separated from the other products, nor can the reaction be controlled sufficiently to provide only the desired products. The propensity of $Mo_2(O\text{-}neo\text{-}Pe)_6$ to react further with the *o*-benzoquinones, especially 9,10-phenanthrenequinone, is most likely the result of the lesser steric requirements of the neopentoxide ligand relative to those of the O-*i*-Pr ligand.[20,21]

$Mo_2(O\text{-}i\text{-}Pr)_6$ + 3 9,10-Phenanthrenequinone. $Mo_2(O\text{-}i\text{-}Pr)_6$ in a solution of methylene chloride and THF reacts with 3 equiv of 9,10-phenanthrenequinone to give a blue-black crystalline product, which is actually a mixture of compounds, regardless of the care taken to obtain only $Mo_2(O\text{-}i\text{-}Pr)_4(O_2C_{14}H_8)_3$. The other products of this reaction are $Mo_2(O\text{-}i\text{-}Pr)_6(O_2C_{14}H_8)_2$ and $Mo_2(O\text{-}i\text{-}Pr)_2(O_2C_{14}H_8)_4$, the relative amounts of which are dependent on the rate of addition of 9,10-phenanthrenequinone.

The ^1H NMR spectrum of $Mo_2(O\text{-}i\text{-}Pr)_4(O_2C_{14}H_8)_3$ can be tentatively assigned by subtraction from the spectrum of resonances associated with the known and isolable compounds $Mo_2(O\text{-}i\text{-}Pr)_6(O_2C_{14}H_8)_2$ and $Mo_2(O\text{-}i\text{-}Pr)_2(O_2C_{14}H_8)_4$. At −65 °C and 360 MHz, ^1H NMR assignments can be made that are consistent with the solid-state structure. The bridging O-*i*-Pr groups, which constitute a doublet at 22 °C, become overlapping doublets centered at δ 2.00 at −65 °C as a result of their diastereotopic nature. The terminal O-*i*-Pr ligands show broad peaks at 22 °C but are resolved at −65 °C to a pair of doublets centered at about δ 1.31 and 0.51. The large chemical shift difference, ca 0.8 ppm, of the diastereotopic methyl groups in the axial O-*i*-Pr ligand can be rationalized in terms of the solid-state structure.

(19) (a) Bradley, D. C.; Westlake, A. H. *Proceedings of the Symposium On Coordination Chemistry*, Tihany, Hungary, 1964; Hungarian Academy of Science: Budapest, Hungary, 1965. (b) Barraclough, C. G.; Bradley, D. C.; Lewis, J.; Thomas, I. M. *J. Chem. Soc.* **1961**, 2601.
(20) (a) Chisholm, M. H.; Huffman, J. C.; Leonelli, J. *J. Chem. Soc., Chem. Commun.* **1981**, 270. (b) Chisholm, M. H.; Huffman, J. C.; Kirkpatrick, C. C.; Leonelli, J. *J. Am. Chem. Soc.* **1981**, *103*, 6093.
(21) Chisholm, M. H.; Folting, K.; Hoffman, D. M.; Huffman, J. C. *J. Am. Chem. Soc.* **1984**, *106*, 6794.

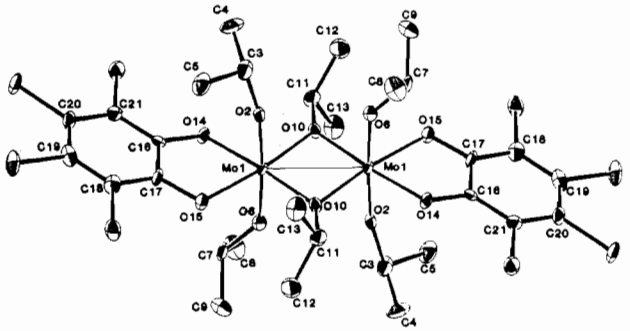

Figure 1. ORTEP view of the $Mo_2(O\text{-}i\text{-}Pr)_6(O_2C_6Cl_4)_2$ molecule showing the atom number scheme used in the tables.

Table III. Fractional Coordinates and Isotropic Thermal Parameters for the $Mo_2(O\text{-}i\text{-}Pr)_6(O_2C_6Cl_4)_2$ Molecule

atom	10^4x	10^4y	10^4z	$10B_{iso}$, Å^2
Mo(1)	5997 (1)	4079 (1)	5297 (1)	10
O(2)	7140 (5)	5286 (5)	6640 (6)	13
C(3)	8176 (8)	5970 (8)	7872 (10)	20
C(4)	8117 (9)	5862 (9)	9361 (10)	26
C(5)	9505 (8)	5502 (9)	7542 (11)	24
O(6)	4929 (5)	2759 (5)	3998 (6)	13
C(7)	4951 (8)	1395 (7)	3534 (9)	16
C(8)	3824 (9)	945 (9)	3849 (11)	25
C(9)	4949 (10)	912 (9)	1881 (10)	27
O(10)	5472 (5)	5066 (5)	3731 (5)	11
C(11)	5961 (8)	5267 (8)	2582 (9)	17
C(12)	5990 (10)	4028 (9)	1378 (10)	26
C(13)	7293 (9)	5802 (9)	3323 (11)	25
O(14)	6669 (5)	3018 (5)	6774 (6)	13
O(15)	7528 (5)	3079 (5)	4550 (6)	13
C(16)	7877 (7)	2475 (7)	6756 (8)	13
C(17)	8341 (8)	2509 (7)	5552 (9)	15
C(18)	9604 (8)	1978 (8)	5479 (9)	18
C(19)	10413 (7)	1446 (7)	6610 (10)	18
C(20)	9947 (8)	1398 (7)	7811 (9)	17
C(21)	8687 (8)	1911 (7)	7866 (8)	14
Cl(22)	10110 (2)	2011 (2)	3958 (2)	19
Cl(23)	12012 (2)	835 (2)	6555 (3)	23
Cl(24)	10967 (2)	758 (2)	9230 (2)	22
Cl(25)	8068 (2)	1870 (2)	9324 (2)	19

The axial O-*i*-Pr ligands each have one methyl oriented along the Mo–(μ-O-*i*-Pr) bond and one methyl oriented along the Mo–O-(catecholate) bond. Thus, one methyl group is directed over the 9,10-phenCat ring system, is shielded by the aromatic π-system, and is shifted upfield (9,10-phenCat = fully reduced form of 9,10-phenanthrenequinone).

Solid-State and Molecular Structures. $Mo_2(O\text{-}i\text{-}Pr)_6(O_2C_6Cl_4)_2$. In the crystalline state this compound is composed of discrete molecules of $Mo_2(O\text{-}i\text{-}Pr)_6(O_2C_6Cl_4)_2$. All hydrogen atoms were located and refined. An ORTEP view of the molecule indicating the coordination geometry and giving the atom-numbering scheme is shown in Figure 1. Fractional coordinates are given in Table III. Listings of pertinent bond distances and angles of non-hydrogen atoms are given in Table IV.

The central $Mo_2O_6(\widehat{O\ O})_2$ unit has virtual D_{2h} symmetry and a crystallographically imposed center of symmetry. Each molybdenum is in a distorted-octahedral geometry with a pair of cis-bridging O-*i*-Pr ligands, a pair of trans-terminal axial O-*i*-Pr ligands, and a pair of cis-terminal equatorial catecholate oxygen atoms.

$Mo_2(O\text{-}neo\text{-}Pe)_6(O_2C_6Cl_4)_2$. This compound is composed of discrete molecules of $Mo_2(O\text{-}neo\text{-}Pe)_6(O_2C_6Cl_4)_2$ in the unit cell. The split crystalline samples used consisted of two crystals, with intensities 80% and 20%. Least-squares refinements were terminated at $R = 0.15$ because the isopropoxy analogue had superior crystals, although the collected data were of sufficient quality to solve the structure.

The central $Mo_2O_6(\widehat{O\ O})_2$ unit exhibits virtual D_{2h} symmetry. Again each molybdenum atom is in a distorted-octahedral geometry oriented exactly as the preceding compound with O-*neo*-Pe ligands substituted for O-*i*-Pr ligands. The bond distances and bond angles differed little from those of the $Mo_2(O\text{-}i\text{-}Pr)_6(O_2C_6Cl_4)_2$ molecule and are given in the supplementary material.

Table IV. Pertinent Bond Distances (Å) and Angles (deg) for the $Mo_2(O\text{-}i\text{-}Pr)_6(O_2C_6Cl_4)_2$ Molecule

Mo(1)–Mo(1)′	2.754 (2)	O(2)–C(3)	1.426 (9)
Mo(1)–O(2)	1.817 (5)	O(6)–C(7)	1.425 (9)
Mo(1)–O(6)	1.844 (5)	O(10)–C(11)	1.446 (9)
Mo(1)–O(10)	2.020 (5)	O(14)–C(16)	1.331 (9)
Mo(1)–O(10)′	2.026 (5)	O(15)–C(17)	1.327 (9)
Mo(1)–O(14)	2.014 (5)	C(16)–C(17)	1.406 (11)
Mo(1)–O(15)	2.016 (5)		

Mo(1)′–Mo(1)–O(2)	91.7 (2)	O(6)–Mo(1)–O(15)	88.1 (2)
Mo(1)′–Mo(1)–O(6)	92.7 (2)	O(10)′–Mo(1)–O(10)	94.2 (2)
Mo(1)′–Mo(1)–O(10)′	47.0 (1)	O(10)–Mo(1)–O(14)	174.4 (2)
Mo(1)′–Mo(1)–O(10)	47.2 (1)	O(10)′–Mo(1)–O(14)	91.4 (2)
Mo(1)′–Mo(1)–O(14)	138.4 (1)	O(10)′–Mo(1)–O(15)	171.6 (2)
Mo(1)′–Mo(1)–O(15)	141.4 (1)	O(10)–Mo(1)–O(15)	94.2 (2)
O(2)–Mo(1)–O(6)	175.4 (2)	O(14)–Mo(1)–O(15)	80.3 (2)
O(2)–Mo(1)–O(10)	91.5 (2)	Mo(1)–O(2)–C(3)	165.1 (5)
O(2)–Mo(1)–O(10)′	90.9 (2)	Mo(1)–O(6)–C(7)	140.1 (5)
O(2)–Mo(1)–O(14)	88.1 (2)	Mo(1)′–O(10)–Mo(1)	85.8 (2)
O(2)–Mo(1)–O(15)	89.2 (2)	Mo(1)′–O(10)–C(11)	134.2 (5)
O(6)–Mo(1)–O(10)	92.3 (2)	Mo(1)–O(10)–C(11)	139.5 (5)
O(6)–Mo(1)–O(10)′	91.3 (2)	Mo(1)–O(14)–C(16)	111.7 (4)
O(6)–Mo(1)–O(14)	87.8 (2)	Mo(1)–O(15)–C(17)	111.9 (5)

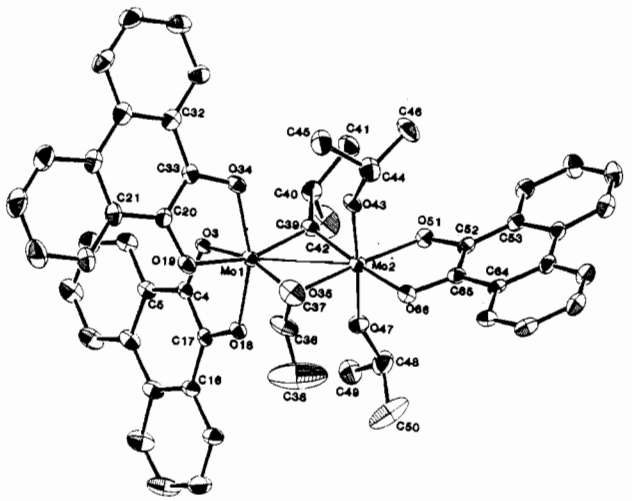

Figure 2. ORTEP view of the $Mo_2(O\text{-}i\text{-}Pr)_4(O_2C_{14}H_8)_3$ molecule giving the atom number scheme used in the tables.

$Mo_2(O\text{-}i\text{-}Pr)_4(O_2C_{14}H_8)_3$. In the solid state the compound $Mo_2(O\text{-}i\text{-}Pr)_4(O_2C_{14}H_8)_3$ contains two molecules per unit cell. The hydrogen atoms were not located but were inserted in calculated positions. The crystals contain two molecules of THF; one is disordered, and both have large thermal parameters. An ORTEP view of the molecule indicating the coordination geometry and the atom-numbering scheme is shown in Figure 2. Fractional coordinates are given in Table V. Listings of pertinent bond distances and angles are given in Table VI.

The $Mo_2O_4(\widehat{O\ O})_3$ unit has virtual C_2 symmetry. Each molybdenum is in a pseudooctahedral geometry with that about Mo(1) being the more distorted from O_h. Mo(1) has a pair of cis-bridging O-*i*-Pr ligands and two terminal 9,10-phenCat ligands, each with one axial and one equatorial catecholate oxygen-to-Mo(1) bond. Mo(2) is disposed in a manner similar to that of the molybdenum atom in the $Mo_2(O\text{-}i\text{-}Pr)_6(O_2C_6Cl_4)_2$ compound, with two cis-bridging O-*i*-Pr ligands, two trans-axial O-*i*-Pr ligands, and a pair of cis-equatorial catecholate oxygen atoms.

Remarks on Structure and Bonding in the $Mo_2(OR)_6(O_2C_6Cl_4)_2$ (R = *i*-Pr, *neo*-Pe) and $Mo_2(O\text{-}i\text{-}Pr)_4(O_2C_{14}H_8)_3$ Molecules. There are three points of interest to be addressed: (1) the observed diamagnetic nature of these compounds, (2) the coordination mode of the *o*-benzoquinone, and (3) a comparison of these compounds to other molecules exhibiting an edge-shared bioctahedral geometry.

Table V. Fractional Coordinates and Isotropic Thermal Parameters for the $Mo_2(O\text{-}i\text{-}Pr)_4(O_2C_{14}H_8)_3$ Molecule

atom	10^4x	10^4y	10^4z	$10B_{iso}$, Å^2	atom	10^4x	10^4y	10^4z	$10B_{iso}$, Å^2
Mo(1)	2290.3 (3)	5865.1 (4)	2877.7 (5)	23	C(41)	2213 (6)	2571 (6)	974 (7)	51
Mo(2)	2063.8 (3)	4623.2 (4)	3898.8 (5)	24	C(42)	928 (6)	3804 (8)	492 (8)	69
O(3)	1858 (2)	6027 (3)	1276 (4)	23	O(43)	3098 (2)	3928 (3)	3981 (4)	27
C(4)	1247 (3)	6853 (5)	1200 (5)	22	C(44)	3822 (4)	3365 (6)	4522 (7)	43
C(5)	910 (3)	7166 (5)	176 (5)	26	C(45)	4488 (4)	3679 (7)	4373 (8)	46
C(6)	1188 (4)	6606 (5)	−830 (6)	31	C(46)	3836 (5)	2163 (7)	3969 (1)	60
C(7)	869 (4)	6933 (6)	−1789 (6)	39	O(47)	1039 (2)	5363 (4)	3765 (4)	31
C(8)	267 (5)	7836 (6)	−1757 (6)	43	C(48)	237 (5)	5500 (7)	3708 (8)	48
C(9)	−24 (4)	8384 (6)	−775 (7)	41	C(49)	−285 (4)	5860 (7)	2692 (8)	47
C(10)	275 (4)	8073 (5)	216 (6)	31	C(50)	107 (6)	6322 (12)	4861 (9)	88
C(11)	−38 (4)	8607 (5)	1253 (6)	31	O(51)	1753 (2)	3220 (3)	3480 (4)	28
C(12)	−707 (5)	9460 (7)	1303 (7)	48	C(52)	1919 (3)	2934 (5)	4448 (5)	26
C(13)	−990 (5)	9937 (7)	2275 (8)	59	C(53)	1872 (4)	1885 (5)	4336 (6)	28
C(14)	−633 (5)	9613 (6)	3251 (7)	45	C(54)	1659 (4)	1074 (6)	3218 (6)	33
C(15)	10 (4)	8785 (5)	3235 (6)	32	C(55)	1628 (4)	61 (6)	3137 (7)	39
C(16)	314 (3)	8271 (5)	2244 (6)	26	C(56)	1817 (5)	−186 (6)	4147 (7)	42
C(17)	969 (3)	7396 (5)	2186 (5)	23	C(57)	2029 (4)	578 (6)	5236 (7)	38
O(18)	1369 (2)	7017 (3)	3059 (4)	24	C(58)	2059 (4)	1631 (5)	5377 (6)	28
O(19)	2971 (2)	6984 (3)	3432 (4)	29	C(59)	2303 (4)	2463 (6)	6526 (6)	30
C(20)	3585 (4)	6612 (5)	2976 (6)	28	C(60)	2511 (4)	2287 (6)	7593 (6)	38
C(21)	4080 (4)	7313 (6)	3125 (6)	34	C(61)	2748 (4)	3052 (7)	8645 (6)	40
C(22)	3916 (5)	8435 (6)	3719 (7)	42	C(62)	2780 (4)	4080 (6)	8721 (6)	37
C(23)	4413 (6)	9091 (7)	3818 (9)	60	C(63)	2586 (4)	4306 (5)	7704 (6)	32
C(24)	5053 (6)	8603 (8)	3355 (10)	65	C(64)	2346 (3)	3503 (5)	6593 (5)	26
C(25)	5218 (5)	7508 (7)	2762 (8)	51	C(65)	2158 (3)	3704 (5)	5519 (6)	26
C(26)	4734 (4)	6805 (6)	2606 (7)	38	O(66)	2214 (2)	4663 (3)	5512 (4)	28
C(27)	4889 (4)	5637 (6)	1977 (6)	35	C(67)	2246 (7)	−138 (8)	674 (10)	18
C(28)	5507 (4)	5111 (7)	1427 (7)	43	C(68)	2068 (9)	−1214 (12)	166 (15)	48
C(29)	5630 (4)	4027 (7)	830 (8)	49	C(69)	2679 (7)	−1797 (12)	592 (12)	91
C(30)	5134 (4)	3396 (6)	722 (7)	43	C(70)	3310 (12)	−1190 (18)	897 (18)	167
C(31)	4520 (4)	3866 (6)	1232 (6)	35	C(71)	2883 (10)	−256 (9)	1180 (12)	28
C(32)	4381 (4)	4988 (6)	1859 (6)	31	C(67)′	3024 (8)	−1311 (11)	−852 (12)	37
C(33)	3740 (4)	5528 (5)	2394 (6)	26	C(68)′	2589 (12)	−1870 (15)	−759 (16)	62
O(34)	3223 (2)	4989 (3)	2344 (4)	27	C(71)′	3225 (14)	−476 (19)	251 (27)	91
O(35)	2432 (2)	6070 (3)	4538 (4)	28	C(72)	3219 (8)	9409 (9)	7332 (11)	83
C(36)	2681 (5)	6886 (6)	5688 (7)	45	C(73)	3914 (9)	9369 (14)	6977 (15)	104
C(37)	3493 (5)	6474 (7)	6280 (7)	49	C(74)	4626 (17)	9355 (18)	7863 (22)	185
C(38)	2110 (8)	7449 (14)	6185 (12)	145	C(75)	4338 (14)	10440 (18)	8650 (18)	150
O(39)	1940 (2)	4454 (3)	2186 (3)	25	C(76)	3715 (19)	10022 (23)	8768 (22)	274
C(40)	1778 (4)	3687 (6)	984 (6)	35					

The observed diamagnetic nature of the compounds and the short Mo-to-Mo distances, 2.754 (2) Å in $Mo_2(O\text{-}i\text{-}Pr)_6(O_2C_6Cl_4)_2$, 2.748 (1) Å in $Mo_2(O\text{-}i\text{-}Pr)_4(O_2C_{14}H_8)_3$, and 2.802 (5) Å in $Mo_2(O\text{-}neo\text{-}Pe)_6(O_2C_6Cl_4)_2$, are consistent with the view that these molecules contain Mo–Mo single bonds. Whenever bridging groups are present, it is not possible to distinguish unequivocally between direct coupling of electron spins via M–M bonding and indirect coupling through bridges.[22,23] However, there exists more than sufficient evidence to support the view that metal–metal bonding is involved. This evidence is as follows:

1. Though Mo–Mo single bonds vary as a function of oxidation state of the metal and ligand character, the distances of 2.748 (1), 2.754 (2), and 2.802 (5) Å for $Mo_2(O\text{-}i\text{-}Pr)_4(O_2C_{14}H_8)_3$, $Mo_2(O\text{-}i\text{-}Pr)_6(O_2C_6Cl_4)_2$, and $Mo_2(O\text{-}neo\text{-}Pe)_6(O_2C_6Cl_4)_2$, respectively, are typical of d^1–d^1 M–M bonding distances for molybdenum.[12a,23]

2. The Mo–Mo distances in these compounds may be compared to those found in the following compounds: (i) $Mo_2(O\text{-}neo\text{-}Pe)_6(M{\equiv}M)$,[11] 2.222 (2) Å; (ii) $Mo_2(O\text{-}i\text{-}Pr)_8(M{=}M)$,[24] 2.523 (1) Å; (iii) $Mo_2(\mu\text{-}CO)(O\text{-}t\text{-}Bu)_6(M{=}M)$,[25] 2.498 (1) Å. Both $Mo_2(O\text{-}i\text{-}Pr)_8$ and $Mo_2(\mu\text{-}CO)(O\text{-}t\text{-}Bu)_6$ have bridging alkoxides.

3. Planar central $Mo_2(\mu\text{-}O)_2$ groups are also found in both $[Mo(O\text{-}i\text{-}Pr)_3(NO)]_2$[26] and $[Mo(O\text{-}i\text{-}Pr)_3(NO)(HNMe_2)]_2$[27] with Mo-to-Mo distances of 3.335 (2) and 3.390 (2) Å, respectively. These have been viewed as nonbonding Mo-to-Mo distances as a result of electronic considerations.

4. Finally, a comparison may be made to group VB alkoxide dimer. Both $[Nb(OMe)_5]_2$[28] and the $Mo_2(OR)_6(O_2C_6Cl_4)_2$ (R = *i*-Pr, *neo*-Pe) and $Mo_2(O\text{-}i\text{-}Pr)_4(O_2C_{14}H_8)_3$ complexes exhibit metal atoms in the +5 oxidation state with octahedral coordination environments. With metal-to-alkoxide oxygen bond distances similar, the focus is directed to the structural parameters of the $M_2(\mu\text{-}O)_2$ units, specifically metal-to-metal distances and the M–O–M bond angles. For $[Nb(OMe)_5]_2$ the averaged[29] Nb–Nb distance is 3.5 Å and the averaged Nb–O–Nb angles are 110°. The Mo-to-Mo distances and Mo–O–Mo angles are 2.78 Å (averaged) and 86.4° (averaged) for the $Mo_2(OR)_6(O_2C_6Cl_4)_2$ and $Mo_2(O\text{-}i\text{-}Pr)_4(O_2C_{14}H_8)_3$ compounds. The shorter metal-to-metal distances and more acute M–O–M angles for the molybdenum system differ from the niobium parameters because these dimers are d^0–d^0 (Nb–Nb) and d^1–d^1 (Mo–Mo), corresponding to bond orders of 0 and 1, respectively. The M–M bond can be easily pictured as a σ-bond arising from overlap to two metal d t_{2g}-type orbitals that bisect the (μ-O)–Mo–(μ-O) angle in octahedral geometry.

Chemical evidence for a metal-to-metal single bond exists as well. $[Nb(OMe)_5]_2$[30] reacts with donor molecules to form mononuclear products of formula $Nb(OMe)_5L$, whereas the $Mo_2(OR)_6(O_2C_6Cl_4)_2$ (R = *i*-Pr, *neo*-Pe) and $Mo_2(O\text{-}i\text{-}Pr)_4(O_2C_{14}H_8)_3$ complexes do not.[31]

(22) Cotton, F. A. *Polyhedron* **1987**, *6*, 667.
(23) Cotton, F. A. *J. Less-Common Met.* **1977**, *54*, 3.
(24) Chisholm, M. H.; Cotton, F. A.; Extine, M. W.; Kelly, R. L. *Inorg. Chem.* **1978**, *17*, 2944.
(25) Chisholm, M. H.; Cotton, F. A.; Extine, M. W.; Kelly, R. L. *J. Am. Chem. Soc.* **1979**, *101*, 7645.
(26) Chisholm, M. H.; Cotton, F. A.; Extine, M. W.; Kelly, R. L. *J. Am. Chem. Soc.* **1978**, *100*, 3354.
(27) Chisholm, M. H.; Huffman, J. C.; Kelly, R. L. *Inorg. Chem.* **1980**, *19*, 2762.
(28) Hubert-Pfalzgraf, L. G.; Pinkerton, A. A.; Reiss, J. G.; Schwarzenbach, D. *Inorg. Chem.* **1976**, *15*, 1196.
(29) Averaged because $[Nb(OMe)_5]_2$ has two conformers in the unit cell.
(30) Hubert-Pfalzgraf, L. G.; Reiss, J. G. *J. Chim. Phys. Phys.-Chim. Biol.* **1973**, *70*, 646.

Table VI. Selected Bond Distances (Å) and Angles (deg) for the $Mo_2(O\text{-}i\text{-}Pr)_4(O_2C_{14}H_8)_3$ Molecule

Mo(1)–Mo(2)	2.7486 (13)	O(3)–C(4)	1.342 (7)
Mo(1)–O(3)	2.021 (4)	O(18)–C(17)	1.326 (7)
Mo(1)–O(18)	1.944 (4)	O(19)–C(20)	1.326 (7)
Mo(1)–O(19)	2.030 (4)	O(34)–C(33)	1.353 (7)
Mo(1)–O(34)	1.941 (4)	O(35)–C(36)	1.459 (8)
Mo(1)–O(35)	1.974 (4)	O(39)–C(40)	1.455 (7)
Mo(1)–O(39)	1.979 (4)	O(43)–C(44)	1.428 (8)
Mo(2)–O(35)	2.045 (4)	O(47)–C(48)	1.418 (9)
Mo(2)–O(39)	2.061 (4)	O(51)–C(52)	1.370 (7)
Mo(2)–O(43)	1.845 (4)	O(66)–C(65)	1.359 (7)
Mo(2)–O(47)	1.840 (4)	C(4)–C(17)	1.368 (8)
Mo(2)–O(51)	1.987 (4)	C(20)–C(33)	1.350 (9)
Mo(2)–O(66)	1.983 (4)	C(52)–C(65)	1.367 (9)
Mo(2)–Mo(1)–O(3)	134.82 (11)	O(35)–Mo(2)–O(43)	88.05 (18)
Mo(2)–Mo(1)–O(18)	99.37 (13)	O(35)–Mo(2)–O(47)	89.69 (19)
Mo(2)–Mo(1)–O(19)	134.33 (13)	O(35)–Mo(2)–O(51)	172.96 (17)
Mo(2)–Mo(1)–O(34)	101.45 (13)	O(35)–Mo(2)–O(66)	91.81 (17)
Mo(2)–Mo(1)–O(35)	47.94 (12)	O(39)–Mo(2)–O(43)	88.47 (17)
Mo(2)–Mo(1)–O(39)	48.39 (12)	O(39)–Mo(2)–O(47)	88.75 (19)
O(3)–Mo(1)–O(18)	76.79 (16)	O(39)–Mo(2)–O(51)	95.17 (17)
O(3)–Mo(1)–O(19)	90.84 (17)	O(39)–Mo(2)–O(66)	175.58 (16)
O(3)–Mo(1)–O(34)	85.96 (17)	O(43)–Mo(2)–O(47)	176.36 (19)
O(3)–Mo(1)–O(35)	162.33 (16)	O(43)–Mo(2)–O(51)	90.52 (18)
O(3)–Mo(1)–O(39)	89.25 (16)	O(43)–Mo(2)–O(66)	88.94 (18)
O(18)–Mo(1)–O(19)	90.54 (17)	O(47)–Mo(2)–O(51)	92.06 (19)
O(18)–Mo(1)–O(34)	158.87 (17)	O(47)–Mo(2)–O(66)	93.98 (18)
O(18)–Mo(1)–O(35)	85.55 (17)	O(51)–Mo(2)–O(66)	81.27 (17)
O(18)–Mo(1)–O(39)	107.76 (17)	Mo(1)–O(3)–C(4)	115.0 (3)
O(19)–Mo(1)–O(34)	77.46 (18)	Mo(1)–O(18)–C(17)	119.4 (4)
O(19)–Mo(1)–O(35)	89.21 (18)	Mo(1)–O(19)–C(20)	113.5 (4)
O(19)–Mo(1)–O(35)	161.20 (17)	Mo(1)–O(34)–C(33)	117.0 (4)
O(34)–Mo(1)–O(35)	111.26 (18)	Mo(1)–O(35)–Mo(2)	86.28 (16)
O(34)–Mo(1)–O(39)	83.98 (17)	Mo(1)–O(35)–C(36)	136.6 (5)
O(35)–Mo(1)–O(39)	96.32 (17)	Mo(2)–O(35)–C(36)	137.2 (5)
Mo(1)–Mo(2)–O(35)	45.79 (12)	Mo(1)–O(39)–Mo(2)	85.72 (15)
Mo(1)–Mo(2)–O(39)	45.90 (11)	Mo(1)–O(39)–C(40)	131.9 (4)
Mo(1)–Mo(2)–O(43)	87.87 (14)	Mo(2)–O(39)–C(40)	142.0 (4)
Mo(1)–Mo(2)–O(47)	88.51 (15)	Mo(2)–O(43)–C(44)	151.7 (4)
Mo(1)–Mo(2)–O(51)	141.06 (12)	Mo(2)–O(47)–C(48)	154.3 (5)
Mo(1)–Mo(2)–O(66)	137.55 (13)	Mo(2)–O(51)–C(52)	112.1 (4)
O(35)–Mo(2)–O(39)	91.68 (17)	Mo(2)–O(66)–C(65)	112.3 (4)

The coordination mode of the *o*-benzoquinone moiety can be considered that of the fully reduced *o*-benzoquinone, i.e. the catecholate dianion, on the basis of infrared spectroscopic data and Mo–O, C–O, and central (between the carbonyl carbons) C–C bond distances associated with the *o*-benzoquinone ligands. (1) Reduction to the catecholate dianion from the respective *o*-benzoquinone effects a shift of ν_{C-O} of $\sim$200 cm^{-1} for $Mo_2(O\text{-}i\text{-}Pr)_4(O_2C_{14}H_8)_3$, $Mo_2(O\text{-}i\text{-}Pr)_6(O_2C_6Cl_4)_2$, and $Mo_2(O\text{-}neo\text{-}Pe)_6(O_2Cl_6Cl_4)_2$. (2) Comparison of the C–O and central C–C distances in $Mo_2(O\text{-}i\text{-}Pr)_4(O_2C_{14}H_8)_3$, $Mo_2(O\text{-}i\text{-}Pr)_6(O_2C_6Cl_4)_2$, and $Mo_2(O\text{-}neo\text{-}Pe)_6(O_2C_6Cl_4)_2$ with those associated with *o*-benzoquinones, *o*-semiquinones, and catecholate ligands (see Table I) indicates the presence of the fully reduced ligands, CAT-2. (3) The Mo–O bond distances are in the range found for Mo–OR bonds, indicating the alkoxide-like nature of the M–O catecholate bonds.[14h]

Finally, with use of the general representation for an edge-shared bioctahedron, depicted in **2**, it has been noted[12b] that the terminal axial bonds are shorter than the terminal equatorial bonds for d^1–d^1 M–M compounds. A comparison of $M–X_a$, $M–X_e$,

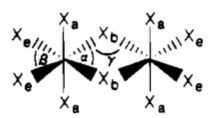

2

$M–X_b$, and M–M distances in addition to α and β angles, presented in Table VII for systems with M–M single bonds, d^1–d^1, and those with no M–M bond, d^0–d^0, reveals several points: (i) The d^1–d^1 systems exhibit a decreased M–M distance, $\sim$0.8 Å, an obtuse α angle, and a decrease in the γ angle. These alterations of the central $M_2(X_b)_2$ core, relative to those in the d^0–d^0 structures, are due to M–M bonding. Also for d^1–d^1 systems the axial substituents bend away from one another, whereas for d^0–d^0 systems they bend toward one another.[32] (ii) The $M–X_b$ distances are longer than M–X terminal distances. (iii) The d^0–d^0 examples show $M–X_a$ and $M–X_e$ distances that are essentially identical. (iv) Examination of $M–X_a$ and $M–X_e$ for the structurally similar $M_2(OR)_6X'_4$ (here X′ = Cl, Br) and $Mo_2(O\text{-}i\text{-}Pr)_6(O_2C_6Cl_4)_2$ compounds shows $M–X_a$ to be ca. 0.1 Å shorter and $M–X_e$ to be longer than those in the appropriate d^0–d^0 systems.[33] The $W_2(O\text{-}i\text{-}Pr)_6(O_2C_2R'_2)_2$ compounds illustrate this long–short analogy particularly well in that there exist $M–X_a$ and $M–X_e$ bonds for both terminal alkoxide and bidentate enediolate ligands and that for each ligand the $M–X_a$ bonds are shorter by ca. 0.1 Å than the $M–X_e$ bonds.[12b] The compound $Mo_2(O\text{-}i\text{-}Pr)_4(O_2C_{14}H_8)_3$ exhibits this "long–short" phenomenon as well, with $M–X_a$ distances again ca. 0.1 Å shorter than for $M–X_e$ for the Mo(1) end of the molecule with two 9,10-phenCat ligands. The molecule also exhibits a very short $M–X_a$ and longer $M–X_e$ for the Mo(2) end of the molecule as previously observed in the $M_2X'_4(OR)_6$ structures.

A qualitative bonding explanation for these "long–short" phenomena proceeds as follows. Consider the coordinate system **3**. The *z* axis has been chosen as coincident with the $X_a–M–X_a$

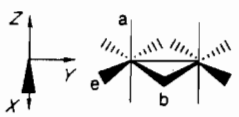

3

bonds. The *x* and *y* axes are assigned such that they bisect the $X_b–M–X_e$ and $X_b–M–X_b$ angles, respectively. This provides $d_{x^2-y^2}$ the appropriate symmetry to form a M–M σ-bond. Thus, the two electrons placed in the molecular orbital derived from two $d_{x^2-y^2}$ interactions exclude this orbital from any π-bonding with donor ligands. The vacant d_{xz} and d_{yz} orbitals are now able to interact most strongly with filled oxygen p orbitals which are perpendicular to the M–O–C plane of the ligand concerned. Inspection of the $M_2X'_4(OR)_6$, $W_2(O\text{-}i\text{-}Pr)_6(O_2C_2R'_2)_2$, and $Mo_2(O\text{-}i\text{-}Pr)_6(O_2C_6Cl_4)_2$ structures show most axial alkoxides with p orbitals aligned to π-donate directly to the d_{xz} or d_{yz} orbitals. The bridging alkoxides and $M–X_e$ O-donors are also oriented such that their p orbitals may also interact with d_{xz} and d_{yz} orbitals to some extent. Therefore, the shortening of the axial bonds in these edge-shared bioctahedral molecules is a result of selective ligand-to-metal π-bonding with the $d_{x^2-y^2}$ orbitals being primarily involved in forming the M–M σ-bond. The elongation of the equatorial bonds occurs despite the fact that X_e atoms are capable of π-bonding into the d_{xz} and d_{yz} orbitals for two reasons: (1) π-Donation into these orbitals, d_{xz} and d_{yz}, would cause X_e to exert a stronger trans influence[34] due to shorter, stronger equatorial bonds, effecting a weakening and lengthening of the $M–X_b$ bonds, leaving a weaker M–M bond. (2) Donor ligands generate stronger $M–X_b$ bonds relative to nondonor ligands.[32] This provides a $M–X_b$ distance in these systems that allows the X_b ligand to compete effectively for π-bonding with X_e. This is borne out by the observation that the $[MCl_5]_2$ compounds (M = Mo, W) have (i) no M–M bond, although they are d^1–d^1, and (ii) a $M–X_b$ distance much longer, relative to $M–X_e$, than those in the corresponding O-donor compounds. This results in giving X_b no opportunity to π-bond; thus, $M–X_a$ and $M–X_e$ have almost identical lengths. It may be con-

(31) $Mo_2(OR)_6(O_2C_6Cl_4)_2$ (R = *i*-Pr, *neo*-Pe) was placed in a ^1H NMR tube in the presence of pyridine-d_5; no change in the ^1H NMR spectrum was observed relative to that obtained in toluene-d_8 or methylene-d_2 chloride.

(32) Fisel, C. R.; Hoffmann, R.; Shaik, S.; Summerville, R. H. *J. Am. Chem. Soc.* **1980**, *102*, 4555.

(33) Mo–O(catecholate) is the same regardless of whether it is X_e or X_a in previously known systems, because when the catecholate compounds are dimeric, they involve Mo(VI) atoms.

(34) Appleton, T. G.; Clark, H. C.; Manzer, L. E. *Coord. Chem. Rev.* **1972**, *10*, 335.

Table VII. Selected Structural Parameters for Edge-Shared Bioctahedral d^0–d^0 and d^1–d^1 Dinuclear Complexes[a]

compd	M–M, Å	α, deg	β, deg	M–X(ax), Å	M–X(eq), Å	M–(μ-X), Å	ref
$[NbCl_5]_2$	3.951 (2)	78.7 (3)	101.2 (3)	2.300 (5)	2.250 (6)	2.555 (6)	*b*
$[MoCl_5]_2$	3.84 (2)	81.4 (1)	96.4 (1)	2.24 (1)	2.25 (1)	2.53 (1)	*c*
$[WCl_5]_2$	3.815 (2)	81.5 (1)	96.3 (2)	2.243 (3)	2.243 (3)	2.519 (3)	*d*
$[Nb(OMe)_5]_2$	3.5	70.4 (3)	104.1 (3)	1.886 (5)	1.904 (9)	2.134 (7)	*e*
$Mo_2(O\text{-}i\text{-}Pr)_6Cl_4$	2.731 (1)	94.7 (1)	85.5 (1)	1.814 (3) [Mo–O]	2.419 (2) [Mo–Cl]	2.014 (3)	*f*
$Mo_2(O\text{-}i\text{-}Pr)_6Br_4$	2.739 (1)	94.3 (2)	83.6 (1)	1.811 (5) [Mo–O]	2.582 (1) [Mo–Br]	2.013 (4) [Mo–O]	*f*
$W_2(OEt)_6Cl_4$	2.715 (1)	95.1 (2)	90.2 (1)	1.824 (4) [W–O]	2.403 (4) [W–Cl]	2.013 (4) [W–O]	*g*
$W_2(O\text{-}i\text{-}Pr)_6(O_2C_2Me_2)_2$	2.754 (2)	96.3 (2)	94.0 (2)	1.92 (1) [α-dik] 1.84 (1) [OR]	2.02 (1) [α-dik] 1.93 (1) [OR]	2.045 (6) 2.045 (6)	*h*
$W_2(O\text{-}i\text{-}Pr)_6(bzl)_2$	2.750 (2)	95.2 (4)	93.0 (4)	1.93 (1) [α-dik] 1.85 (1) [OR]	2.02 (1) [α-dik] 1.93 (1) [OR]	1.99 (1) 1.99 (1)	*h*
$Mo_2(O\text{-}i\text{-}Pr)_6(O_2C_6Cl_4)_2$	2.754 (2)	94.2 (2)	80.3 (2)	1.831 (5) [Mo–OR]	2.015 (5) [Q]	2.023 (5)	this work
$Mo_2(O\text{-}neo\text{-}Pe)_6(O_2C_6Cl_4)_2$	2.802 (2)	93.1 (5)	80.8 (5)	1.860 (16)	2.010 (14) [Q]	2.038 (14)	this work
$Mo_2(O\text{-}i\text{-}Pr)_4(O_2C_{14}H_8)_3$	2.7486 (13)	96.32 (17)	81.27 (17) [Q]	1.843 (4) [OR]	1.985 (4) [Q]	1.977 (4) [Mo(1)–OR]	this work
			90.84 (17) [2Q]	1.943 (4) [2Q]	2.026 (4) [2Q]	2.053 (4) [Mo(2)–OR]	this work

[a] Angles are defined by $\alpha = X_b\text{–}M\text{–}X_b$ and $\beta = X_e\text{–}M\text{–}X_e$, as defined in **2** in the text. [b] Zalkin, A.; Sands, D. D. *Acta Crystallogr.* **1958**, *11*, 615. [c] Sands, D. D.; Zalkin, A. *Acta Crystallogr.* **1959**, *12*, 723. [d] Cotton, F. A.; Rice, C. E. *Acta Crystallogr., Sect. B: Struct. Crystallogr. Cryst. Chem.* **1978**, *B34*, 2833. [e] Pinkerton, A. A.; Schwarzenbach, D.; Hubert-Pfalzgraf, L. G.; Reiss, J. G. *Inorg. Chem.* **1976**, *15*, 1196. [f] Chisholm, M. H.; Huffman, J. C.; Kirkpatrick, C. C. *Inorg. Chem.* **1981**, *20*, 871. [g] Cotton, F. A.; Walton, R. A.; DeMarco, D.; Kolthammer, B. S. W. *Inorg. Chem.* **1981**, *20*, 3048. [h] Chisholm, M. L.; Huffman, J. C.; Ratermann, A. L. *Inorg. Chem.* **1983**, *22*, 4100. bzl = benzil.

cluded, then, that M–M σ, L–M π, and $M_2(X_b)_2$ core binding effects favor short axial and long equatorial M–X bonds for these M–M singly bonded systems.

$Mo_2(O\text{-}i\text{-}Pr)_8$ + 2 $O_2C_6Cl_4$. Midnight blue solutions of $Mo_2(O\text{-}i\text{-}Pr)_8$ turn black-violet upon addition of tetrachloro-1,2-benzoquinone. The solution produces blackish crystals of $Mo_2(O\text{-}i\text{-}Pr)_6(O_2C_6Cl_4)_2$ overnight as determined by ^1H NMR. Small-scale reactions of $Mo_2(O\text{-}i\text{-}Pr)_8$ and tetrachloro-1,2-benzoquinone carried out so as to trap any volatile compounds or side products of the reaction show the byproducts of this reaction to be 2-propanol and acetone. These products are indicative of $^{\bullet}O\text{-}i\text{-}Pr$ formation. Alkoxide radical formation is also implied in the reactions of $Mo_2(O\text{-}i\text{-}Pr)_6$ with greater than 2 equiv of *o*-benzoquinones (vide infra).

$Mo_2(OR)_6$ (R = *i*-Pr, *neo*-Pe) + 4*o*-quin (*o*-quin = Tetrachloro-1,2-benzoquinone, 9,10-Phenanthrenequinone). Upon reaction with either tetrachloro-1,2-benzoquinone or 9,10-phenanthrenequinone yellow methylene chloride solutions of $Mo_2(OR)_6$ (R = *i*-Pr, *neo*-Pe) turn immediately to a black-violet. These dark solutions produce the black crystalline solids $Mo_2(OR)_2(O_2C_{14}H_8)_4$ and $Mo_2(OR)_2(O_2C_6Cl_4)_4$, for R = *i*-Pr, *neo*-Pe. All four compounds are air- and water-sensitive. Inspection of the infrared spectra shows a shift in the $\nu_{C\text{–}O}$ band, relative to that of the parent *o*-benzoquinone, of ca. 200 cm^{-1}. This is indicative of catecholate formation, a formal 2e reduction of the parent *o*-benzoquinone. The region of the infrared spectra containing $\nu_{M\text{–}O}$, 500–630 cm^{-1}, shows absorbances suggestive of doubly bridging alkoxides[19] in addition to $\nu_{M\text{–}O}$ consistent with the presence of a terminal catecholate ligand.[35]

The ^1H NMR spectra of $Mo_2(O\text{-}neo\text{-}Pe)_2(O_2C_{14}H_8)_4$ and $Mo_2(O\text{-}neo\text{-}Pe)_2(O_2C_6Cl_4)_4$ are extremely similar to the neopentyl region. At 22 °C both compounds give a sharp singlet for the CMe_3 group of neopentoxide, δ 0.86 for $Mo_2(O\text{-}neo\text{-}Pe)_2(O_2C_6Cl_4)_4$, δ 1.05 for $Mo_2(O\text{-}neo\text{-}Pe)_2(O_2C_{14}H_8)_3$, and a broad peak downfield for the methylene protons of the O-*neo*-Pe ligands. At −50 °C the CMe_3 singlets are undisturbed but the broad methylene peaks for $Mo_2(O\text{-}neo\text{-}Pe)_2(O_2C_{14}H_8)_4$ and $Mo_2(O\text{-}neo\text{-}Pe)_2(O_2C_6Cl_4)$ have become AB quartets positioned at about δ 4.99 and 4.95, respectively. A parallel situation exists for the $Mo_2(O\text{-}i\text{-}Pr)_2(O_2C_6Cl_4)_4$ and $Mo_2(O\text{-}i\text{-}Pr)_2(O_2C_{14}H_8)_4$ compounds. Room-temperature spectra reveal a doublet for the isopropyl methyls at δ 1.58 with a methine resonance at δ 5.85. At −65 °C the methine protons are unshifted but the isopropyl methyls have become inequivalent, giving overlapping doublets at δ 1.53. The aromatic region of the spectra for the 9,10-phenCat-containing compounds show a doublet and triplet with broad peaks between them at 22 °C that sharpen at lower temperatures to give resonances interpretable by the following model. A solid-state structure such as **4** is consistent with the low-temperature spectra

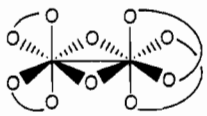

4

for all four molecules. The methylenes of the O-*neo*-Pe ligands and the methyl groups of the O-*i*-Pr ligands would be diastereotopic. The resonances of the 9,10-phenCat protons should potentially show four doublets and four triplets. This is consistent with the observed low-temperature spectra in the aromatic region. When the temperature is raised to 22 °C, the bridging alkoxide resonances lose their respective diastereotopic nature and the aromatic region reverts to a doublet and a triplet with broad peaks between them. This dynamic behavior may be explained in terms of concerted trigonal twists at adjacent trigonal faces (Bailar twist mechanism at an edge-shared bioctahedron) or by rhombic twists (Ray and Dutt) at the dinuclear center.

$W_2(O\text{-}i\text{-}Pr)_6L_2$ + 2 9,10-Phenanthrenequinone (L = $HNMe_2$, py). Toluene solutions of either $W_2(O\text{-}i\text{-}Pr)_6(HNMe_2)_2$ or $W_2(O\text{-}i\text{-}Pr)_6(py)_2$ react slowly with 9,10-phenanthrenequinone. There is no dramatic color change as the reaction proceeds, although the shade of red for the reactant material is subtly different from that of the product. The reaction appears to be faster for L = dimethylamine than for L = pyridine. The final products are the same for both adducts of the $W_2(O\text{-}i\text{-}Pr)_6$ moiety, namely a mixture of $W_2(O\text{-}i\text{-}Pr)_6(O_2C_{14}H_8)_2$, $W_2(O\text{-}i\text{-}Pr)_4(O_2C_{14}H_8)_3$, $W_2(O\text{-}i\text{-}Pr)_2(O_2C_{14}H_8)_4$, and some starting material.

The ^1H NMR spectrum shows five (excluding starting material) isopropyl methyl doublets at 22 °C. On the basis of knowledge of the molybdenum analogues the peaks may be reasonably assigned. Methyl resonances at δ 0.68 and 2.15 are in the integral ratio 2:1, consistent with the formulation $W_2(O\text{-}i\text{-}Pr)_6(O_2C_{14}H_8)_2$. The respective methine resonances are at δ 5.07 and 6.66. The $W_2(O\text{-}i\text{-}Pr)_2(O_2C_{14}H_8)_4$ product exhibits a methyl doublet at δ 1.25 with the methine septet located at δ 5.60. Finally, for the $W_2(O\text{-}i\text{-}Pr)_4(O_2C_{14}H_8)_3$ molecule, isopropyl methyl doublets are found at δ 1.08 and 1.61 in the ratio 1:1 with methines at δ 4.93 and 7.10. The assignments in this spectra are fairly certain, though the assignment of the methines at δ 5.07 and 4.93 could be switched. These two methine resonances for the terminal O-*i*-Pr ligands in $W_2(O\text{-}i\text{-}Pr)_4(O_2C_{14}H_8)_3$ and $W_2(O\text{-}i\text{-}Pr)_6(O_2C_{14}H_8)_2$ are likewise adjacent in the molybdenum analogues, and their relative positions have been assigned on the basis of the molybdenum spectra.

(35) There exist no assignments of $\nu_{Mo\text{–}O}$ for catecholates; however, inspection of those papers that include IR data suggest $\nu_{Mo\text{–}O}$ to be in the same area as $\nu_{Mo\text{–}O}$ for alkoxides.

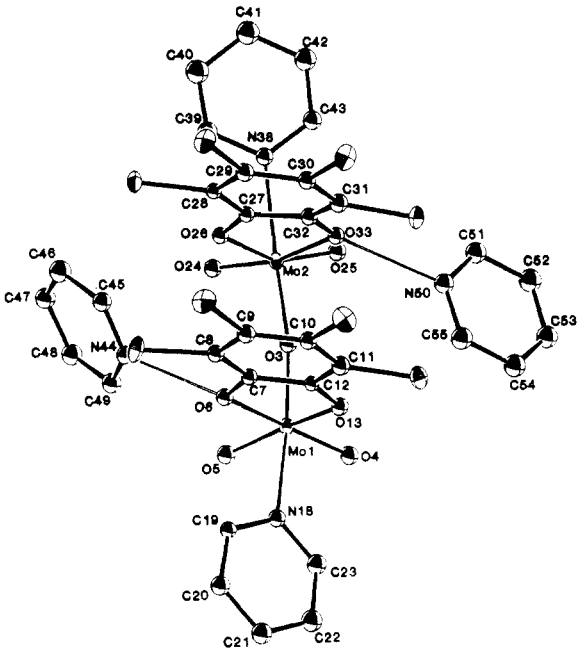

Figure 3. ORTEP view of the $[pyH]_2[(MoO_2(O_2C_6Cl_4)py)_2O]$ molecule showing the atom number scheme used in the tables.

Efforts to obtain $W_2(O\text{-}i\text{-}Pr)_6(O_2C_{14}H_8)_2$ in a pure state were unsuccessful. A plausible explanation for the observed difference between the chemistry of the $M_2(OR)_6$ compounds where M = Mo versus that for M = W can be offered. It is known that tungsten binds Lewis bases more strongly and, except for $W_2(O\text{-}t\text{-}Bu)_6$, the other alkoxides employed here are introduced as the Lewis base adducts $W_2(OR)_6L_2$.[11b,36] Lewis base dissociation may well be required for reactions with *o*-quinones. However, it is also easier to oxidize W_2 centers relative to Mo_2 centers[37] and subsequent attack by *o*-quinone ligands on $M_2(OR)_6(O\frown O)_2$ may occur more readily for M = W than for M = Mo. If this is true, then a distribution of products will always be favored for tungsten.

$Mo_2(O\text{-}t\text{-}Bu)_6$ + 2 $O_2C_6Cl_4$. In the absence of pyridine the reaction of $Mo_2(O\text{-}t\text{-}Bu)_6$ with tetrachloro-1,2-benzoquinone in THF affords a blue solution. From this solution small blue plates can be grown after layering the solution with methylene chloride. The ^1H NMR spectrum shows resonances indicative of uncoordinated THF. The infrared spectrum indicates a compound with coordinated tetrachlorocatecholate or tetrachlorosemiquinone and no O-*t*-Bu ligands. This information in conjunction with the elemental analysis and cryoscopic molecular weight determination suggest a compound of formula $Mo_2O_5(O_2C_6Cl_4)_2\cdot 4THF$.[38]

The blue compound reacts with pyridine, at least 4 equiv, to produce red crystals of $[(MoO_2(O_2C_6Cl_4)py)_2O][pyH]_2$. This compound shows only coordinated pyridine in the ^1H NMR spectrum. The infrared spectrum has strong absorbances at 908 and 895 cm^{-1} indicative of the cis MoO_2 groups. The presence of absorbances assignable to ν_{sym} at 775 cm^{-1} and ν_{as} at 585 cm^{-1} are consistent with a nonlinear M–O–M arrangement.[39] The rest of the spectrum is consistent with the presence of pyridne, $\nu_{C=C}$ 1600 cm^{-1}, and coordinated catecholate ligands on the basis of ν_{C-O} shifts and the presence of ν_{M-O} at 593 cm^{-1}.

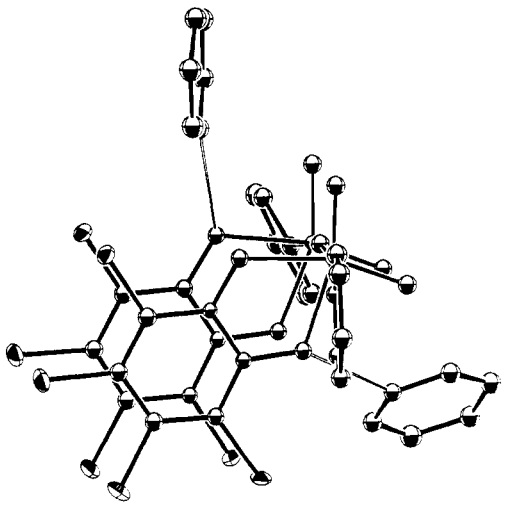

Figure 4. ORTEP view of $[pyH]_2[(MoO_2(O_2C_6Cl_4)py)_2O]$ down the Mo–O–Mo bond, emphasizing the eclipsed nature of the cis oxo and tetrachlorocatecholate groups on each end of the molecule.

Solid-State Structure of $[pyH]_2[(MoO_2(O_2C_6Cl_4)py)_2O]$. The molecule $[pyH]_2[(MoO_2(O_2C_6Cl_4)py)_2O]$ crystallized from a THF/pyridine solution in the space group $P2_1/c$ with eight molecules in the unit cell. The ORTEP views are given in Figures 3 and 4. Figure 3 shows the coordination geometry and gives the atom-numbering scheme. Figure 4 indicates the nearly eclipsed nature of the terminal oxo and tetrachlorocatecholate groups. Atomic positional parameters are given in Table VIII. Listings of pertinent bond distances and angles are given in Tables IX and X, respectively.

This molecule exhibits virtual C_{2v} symmetry. Each molybdenum is in a distorted-octahedral geometry with (1) a pair of cis oxo ligands, (2) two cis catecholate oxygens, and (3) a pyridine trans to the oxo bridge. The Mo–O_b–Mo angle is 168.7 (4)°. There exist two pyridinium cations hydrogen-bonded to one catecholate oxygen atom on each end of the molecule in a transoid arrangement.

Structure and Bonding in $[pyH]_2[Mo_2O_5(O_2C_6Cl_4)_2(py)_2]$. The $[Mo_2O_5(O_2C_6Cl_4)_2(py)_2]^{2-}$ molecule is a member of a family of Mo(VI) compounds that exhibit a single oxo bridge connecting the two Mo atoms.[40] In this class of compounds there exists a large range of Mo–O–Mo angles, from strictly 180° in $Mo_2O_5(C_2O_4)_2(H_2O)_2^{2-}$[40b] to 136° in $Mo_2O_3(O_2)_2(H_2O)_2^{2-}$.[40d] The Mo–O–Mo linkage in the $[Mo_2O_5(O_2C_6Cl_4)_2(py)_2]^{2-}$ anion has an angle of 168.7 (4)°. This angle is very close to that in $Mo_2O_5(dmf)_4Cl_2$ (171°),[40c] which is considered to be an intermediate value.[40a,f,g]

The bridging Mo–O distances are crystallographically the same, being 1.893 (7) and 1.896 (8) Å for Mo(1)–O(3) and Mo(2)–O(3), respectively. These distances are comparable to those in other compounds that contain the $Mo_2O_5^{2+}$ core.[40]

The four terminal Mo–oxo bonds have an average distance of 1.720 (13) Å, consistent with distances in $Mo_2O_5^{2+}$ complexes and mononuclear complexes with MoO_2^{2+} core structures. The angle subtended at Mo involving the cis oxo groups is 106.0 (7)°, which is expected to be >90° due to O···O repulsion between tightly bound oxo ligands.[41]

(36) Chetcuti, M. J.; Chisholm, M. H.; Huffman, J. C.; Leonelli, J. *J. Am. Chem. Soc.* **1983**, *105*, 292.
(37) (a) Chisholm, M. H.; Huffman, J. C.; Smith, C. A. *J. Am. Chem. Soc.* **1986**, *108*, 222. (b) Akiyama, M.; Chisholm, M. H.; Cotton, F. A.; Extine, M. W.; Haitko, D. A.; Leonelli, J.; Little, D. *J. Am. Chem. Soc.* **1981**, *103*, 779.
(38) (a) Buchanan, R. M.; Pierpont, C. G. *Inorg. Chem.* **1982**, *21*, 652. (b) Buchanan, R. M.; Pierpont, C. G. *J. Am. Chem. Soc.* **1975**, *97*, 6450.
(39) (a) Cotton, F. A.; Wing, R. M. *Inorg. Chem.* **1965**, *4*, 867. (b) Griffith, W. P. *J. Chem. Soc. A* **1969**, 211. (c) Griffith, W. P.; Hewkin, D. J. *J. Chem. Soc. A* **1966**, 472. (d) Callahan, K. P.; Wing, R. M. *Inorg. Chem.* **1969**, *6*, 871.
(40) (a) Bruce, A. E.; Corbin, J. L.; Enemark, J. H.; Marabella, C. P.; Miller, K. F.; Pariyadth, N.; Stiefel, E. I. *Inorg. Chem.* **1983**, *22*, 3456. (b) Cotton, F. A.; Morehouse, S. M.; Wood, J. S. *Inorg. Chem.* **1964**, *3*, 1603. (c) Atovmyan, L. O.; Sokovova, Y. A.; Thackey, V. V. *Dokl. Akad. Nauk SSSR* **1970**, *195*, 1355. (d) Stomberg, R. *Acta Chem. Scand.* **1968**, *22*, 1076. (e) Carpentier, J. M.; Mitschler, A.; Weiss, R. *Acta Crystallogr., Sect. B: Struct. Crystallogr. Cryst. Chem.* **1972**, *B28*, 1288. (f) Rodier, N. A.; Viossat, B. *Acta Crystallogr., Sect. B: Struct. Crystallogr. Cryst. Chem.* **1981**, *B37*, 56. (g) Knobler, C.; Penfold, B. R.; Robinson, W. T.; Willeins, C. J.; Yong, S. H. *J. Chem. Soc., Dalton Trans.* **1980**, 248. (h) Matheson, A. J.; Penfold, B. R. *Acta Crystallogr., Sect. B: Struct. Crystallogr. Cryst. Chem.* **1979**, *B35*, 2707. (i) Knobler, C. B.; Robinson, W. T.; Wilkins, C. J.; Wilson, A. J. *Acta Crystallogr., Sect. C: Cryst. Struct. Commun.* **1983**, *C39*, 443.

Table VIII. Fractional Coordinates and Isotropic Thermal Parameters for $[pyH]_2[(MoO_2(O_2C_6Cl_4)py)_2O]$

atom	10^4x	10^4y	10^4z	$10B_{iso}$, Å^2	atom	10^4x	10^4y	10^4z	$10B_{iso}$, Å^2
Mo(1)	7908.8 (3)	4215 (1)	7223.5 (5)	14	Mo(1)′	7272.5 (3)	−754 (1)	7631.7 (5)	11
Mo(2)	8701.9 (3)	3956 (1)	5832.0 (5)	13	Mo(2)′	6410.0 (3)	−1112 (1)	8875.1 (5)	12
O(3)	8261 (2)	4045 (6)	6457 (4)	21 (1)	O(3)′	6833 (2)	−1046 (5)	8223 (4)	15 (1)
O(4)	7473 (2)	4761 (6)	6755 (4)	20 (1)	O(4)′	7437 (2)	−1927 (5)	7423 (4)	16 (1)
O(5)	7758 (2)	3007 (6)	7374 (4)	22 (1)	O(5)′	7659 (2)	−295 (5)	8286 (4)	16 (1)
O(6)	8430 (2)	3940 (5)	8075 (4)	14 (1)	O(6)′	7005 (2)	712 (5)	7509 (4)	14 (1)
C(7)	8581 (3)	4756 (8)	8441 (6)	14 (2)	C(7)′	6697 (3)	837 (8)	6956 (5)	12 (2)
C(8)	8852 (3)	4731 (8)	9098 (6)	13 (2)	C(8)′	6476 (3)	1726 (8)	6806 (6)	14 (2)
C(9)	8978 (3)	5607 (8)	9461 (6)	18 (2)	C(9)′	6163 (3)	1778 (8)	6214 (6)	16 (2)
C(10)	8827 (3)	6526 (8)	9180 (6)	17 (2)	C(10)′	6085 (3)	972 (8)	5732 (6)	15 (2)
C(11)	8559 (3)	6554 (8)	8505 (6)	14 (2)	C(11)′	6316 (3)	98 (8)	5864 (6)	17 (2)
C(12)	8437 (3)	5665 (8)	8147 (5)	12 (2)	C(12)′	6622 (3)	17 (7)	6484 (5)	11 (2)
O(13)	8162 (2)	5624 (5)	7527 (4)	15 (1)	O(13)′	6851 (2)	−804 (5)	6655 (4)	15 (1)
Cl(14)	9007 (1)	3580 (2)	9465 (1)	23	Cl(14)′	6601 (1)	2739 (2)	7387 (1)	20
Cl(15)	9309 (1)	5576 (2)	10279 (1)	21	Cl(15)′	5870 (1)	2880 (2)	6059 (2)	23
Cl(16)	8969 (1)	7631 (2)	9633 (1)	19	Cl(16)′	5715 (1)	1067 (2)	4970 (2)	24
Cl(17)	8353 (1)	7674 (2)	8147 (1)	17	Cl(17)′	6245 (1)	−917 (2)	5268 (1)	19
N(18)	7581 (3)	4561 (7)	8257 (5)	17 (2)	N(18)′	7713 (3)	−120 (6)	6816 (5)	15 (2)
C(19)	7615 (4)	3962 (9)	8848 (6)	21 (2)	C(19)′	7763 (3)	886 (8)	6726 (5)	13 (2)
C(20)	7420 (4)	4136 (10)	9481 (7)	29 (2)	C(20)′	8039 (3)	1272 (8)	6264 (6)	18 (2)
C(21)	7165 (4)	4983 (10)	9487 (7)	34 (3)	C(21)′	8281 (4)	660 (9)	5865 (6)	21 (2)
C(22)	7120 (4)	5627 (9)	8870 (7)	27 (2)	C(22)′	8225 (4)	−389 (9)	5958 (6)	22 (2)
C(23)	7342 (4)	5404 (8)	8263 (6)	20 (2)	C(23)′	7953 (3)	−740 (8)	6439 (6)	19 (2)
O(24)	8752 (2)	2687 (5)	5764 (4)	17 (1)	O(24)′	6684 (2)	−662 (5)	9674 (4)	15 (1)
O(25)	8439 (2)	4365 (5)	5008 (4)	15 (1)	O(25)′	6382 (2)	−2400 (5)	8974 (4)	16 (1)
O(26)	9167 (2)	3939 (5)	6742 (4)	18 (1)	O(26)′	6146 (2)	299 (5)	8656 (4)	13 (1)
C(27)	9284 (3)	4811 (8)	7059 (6)	13 (2)	C(27)′	5830 (3)	398 (7)	8098 (5)	12 (2)
C(28)	9550 (3)	4913 (8)	7703 (5)	12 (2)	C(28)′	5606 (3)	1281 (7)	7948 (5)	12 (2)
C(29)	9643 (3)	5851 (8)	8005 (6)	16 (2)	C(29)′	5295 (3)	1337 (8)	7336 (6)	16 (2)
C(30)	9462 (3)	6710 (8)	7667 (5)	12 (2)	C(30)′	5234 (3)	503 (8)	6877 (6)	15 (2)
C(31)	9197 (3)	6610 (8)	7007 (6)	15 (2)	C(31)′	5458 (3)	−376 (8)	7037 (6)	16 (2)
C(32)	9103 (3)	5667 (7)	6697 (5)	11 (2)	C(32)′	5735 (3)	−443 (8)	7668 (6)	14 (2)
O(33)	8852 (2)	5509 (5)	6068 (4)	13 (1)	O(33)′	5952 (2)	−1278 (5)	7902 (4)	14 (1)
Cl(34)	9753 (1)	3843 (2)	8152 (1)	23	Cl(34)′	5696 (1)	2302 (2)	8536 (1)	17
Cl(35)	9973 (1)	5963 (2)	8830 (1)	19	Cl(35)′	5003 (1)	2414 (2)	7157 (2)	21
Cl(36)	9565 (1)	7868 (2)	8056 (2)	22	Cl(36)′	4849 (1)	560 (2)	6110 (1)	23
Cl(37)	8971 (1)	7655 (2)	6556 (1)	21	Cl(37)′	5400 (1)	−1375 (2))	6426 (1)	18
N(38)	9296 (3)	4009 (6)	5213 (4)	13 (2)	N(38)′	5829 (3)	−1132 (6)	9545 (5)	15 (2)
C(39)	9590 (3)	3276 (8)	5316 (6)	18 (2)	C(39)′	5769 (3)	−368 (8)	10019 (6)	18 (2)
C(40)	9914 (4)	3155 (9)	4885 (6)	20 (2)	C(40)′	5464 (4)	−406 (9)	10495 (7)	26 (2)
C(41)	9942 (3)	3830 (9)	4315 (6)	20 (2)	C(41)′	5189 (4)	−1262 (9)	10502 (7)	25 (2)
C(42)	9651 (4)	4607 (9)	4197 (7)	27 (2)	C(42)′	5252 (4)	−2026 (9)	10001 (6)	23 (2)
C(43)	9335 (4)	4675 (9)	4664 (7)	24 (2)	C(43)′	5569 (3)	−1946 (8)	9537 (6)	17 (2)
N(44)	8784 (4)	2113 (9)	7829 (6)	36 (2)	N(44)′	7105 (3)	1389 (6)	8978 (5)	15 (2)
C(45)	9068 (4)	1824 (10)	7374 (7)	29 (2)	C(45)′	6773 (3)	1840 (8)	9204 (6)	17 (2)
C(46)	9118 (4)	780 (10)	7277 (7)	29 (2)	C(46)′	6756 (4)	2058 (9)	9946 (6)	23 (2)
C(47)	8878 (4)	121 (9)	7648 (6)	22 (2)	C(47)′	7097 (4)	1774 (8)	10435 (6))	20 (2)
C(48)	8597 (4)	485 (9)	8109 (7)	24 (2)	C(48)′	7447 (4)	1270 (9)	10189 (6)	21 (2)
C(49)	8545 (4)	1503 (11)	8189 (8)	37 (3)	C(49)′	7445 (3)	1109 (8)	9442 (6)	19 (2)
N(50)	8076 (3)	6382 (7)	5603 (5)	21 (2)	N(50)′	6148 (3)	−2998 (7)	7289 (5)	18 (2)
C(51)	7971 (4)	6484 (9)	4868 (6)	22 (2)	C(51)′	6024 (4)	−3837 (9)	7626 (6)	21 (2)
C(52)	7599 (4)	6945 (8)	4600 (6)	20 (2)	C(52)′	6168 (4)	−4781 (9)	7376 (7)	24 (2)
C(53)	7325 (3)	7286 (8)	5093 (6)	19 (2)	C(53)′	6416 (4)	−4767 (9)	6791 (6)	23 (2)
C(54)	7436 (4)	7168 (9)	5856 (6)	21 (2)	C(54)′	6522 (4)	−3905 (9)	6451 (6)	23 (2)
C(55)	7823 (4)	6713 (9)	6101 (6)	21 (2)	C(55)′	6386 (4)	−3003 (9)	6713 (6)	23 (2)

The remaining ligands are the tetrachlorocatecholate moiety and pyridine. The pyridine ligands are trans to the bridging oxo ligand with an average Mo–N distance of 2.301 (12) Å, which is consistent with pyridine acting as a simple donor ligand.[42] The tetrachlorocatecholate has C–C and C–O distances of 1.397 (18) and 1.342 (16) Å, respectively. These bond lengths support the view of a 2e reduction of the parent *o*-benzoquinone to give a catecholate ligand. The M–O catecholate distances are crystallographically different, 2.094 (10) and 2.16 (1) Å (averaged), with the oxygen atom of the longer Mo–O bond being involved in hydrogen bonding to the pyridinium cation.

Finally, it should be noted that the respective MoO_2 moieties adopt an eclipsed structure relative to one another when viewed down the Mo–O–M axis (see Figure 4) whereas other compounds containing the $M_2O_5^{2+}$ core with a single oxo bridge exist in the trans or anti conformation.[40a–c] For the complexes of Enemark, Stiefel, et al.,[40a] the trans or anti conformation is probably a result of a molecular arrangement that provides maximum intramolecular hydrogen bonding between the central NH group of the ligand coordinated to one molybdenum atom and the terminal oxo group on the other molybdenum atom. In fact, their Mo–O–Mo angles are smaller than expected as a result of this intramolecular hydrogen bonding.

The eclipsed nature of the oxo groups on the $Mo_2O_5^{2+}$ moiety finds its origin with the tetrachlorocatecholate ligands. Inter- and intramolecular interactions of ring systems in a variety of reduced *o*-benzoquinone (SQ-1, CAT-2) complexes have been observed.[6,43]

(41) This phenomenon is common; see ref 40a–c,f,i and: Cotton, F. A.; Elder, R. C. *Inorg. Chem.* **1964**, *3*, 397.
(42) See ref 14h and 40a,b.
(43) Quinones are well-known for their ability to form charge-transfer complexes with other planar unsaturated organic molecules: (a) Foster, R. *Organic Charge Transfer Complexes*; Academic: London, 1969. (b) Foreman, M. I.; Foster, R. In *The Chemistry of Quinonoid Complexes*; Patai, S., Ed.; Wiley: New York, 1974.

Table IX. Selected Bond Distances (Å) for the $[pyH]_2[(MoO_2(O_2C_6Cl_4)py)_2O]$ Molecule

Bond Distances			
Mo(1)–O(3)	1.893 (7)	Mo(2)′–O(3)′	1.885 (7)
Mo(1)–O(4)	1.703 (7)	Mo(2)′–O(24)′	1.717 (7)
Mo(1)–O(5)	1.713 (8)	Mo(2)′–O(25)′	1.735 (7)
Mo(1)–O(6)	2.167 (7)	Mo(2)′–O(26)′	2.084 (7)
Mo(1)–O(13)	2.097 (7)	Mo(2)′–O(33)′	2.174 (7)
Mo(1)–N(18)	2.292 (9)	Mo(2)′–N(38)′	2.314 (9)
Mo(2)–O(3)	1.896 (8)	O(6)–C(7)	1.339 (12)
Mo(2)–O(24)	1.708 (7)	O(13)–C(12)	1.347 (12)
Mo(2)–O(25)	1.723 (7)	O(26)–C(27)	1.336 (12)
Mo(2)–O(26)	2.091 (7)	O(33)–C(32)	1.336 (11)
Mo(2)–O(33)	2.163 (7)	O(6)′–C(7)′	1.332 (12)
Mo(2)–N(38)	2.293 (8)	O(13)′–C(12)′	1.332 (12)
Mo(1)′–O(3)′	1.889 (7)	O(26)′–C(27)′	1.351 (12)
Mo(1)′–O(4)′	1.708 (7)	O(33)′–C(32)′	1.354 (12)
Mo(1)′–O(5)′	1.724 (7)	C(7)–C(12)	1.386 (14)
Mo(1)′–O(6)′	2.136 (7)	C(27)–C(32)	1.410 (14)
Mo(1)′–O(13)′	2.104 (7)	C(7)′–C(12)′	1.397 (14)
Mo(1)′–N(18)′	2.305 (9)	C(27)′–C(32)′	1.384 (14)
Distances Involving Hydrogen Bonding			
N(44)–O(6)	2.743	N(44)′–O(6)′	2.808
N(50)–O(33)	2.765	N(50)′–O(33)′	2.658

Table X. Selected Bond Angles (deg) for the $[pyH]_2[(MoO_2(O_2C_6Cl_4)py)_2O]$ Molecule

O(3)–Mo(1)–O(4)	101.0 (3)	O(3)′–Mo(1)′–O(5)′	100.9 (3)
O(3)–Mo(1)–O(5)	101.6 (3)	O(3)′–Mo(1)′–O(6)′	86.68 (28)
O(3)–Mo(1)–O(6)	92.6 (3)	O(3)′–Mo(1)′–O(13)′	92.14 (28)
O(3)–Mo(1)–O(13)	93.6 (3)	O(3)′–Mo(1)′–N(18)′	167.6 (3)
O(3)–Mo(1)–N(18)	170.1 (3)	O(4)′–Mo(1)′–O(5)′	105.7 (3)
O(4)–Mo(1)–O(5)	105.1 (4)	O(4)′–Mo(1)′–O(6)′	161.0 (3)
O(4)–Mo(1)–O(6)	160.2 (3)	O(4)′–Mo(1)′–O(13)′	87.9 (3)
O(4)–Mo(1)–O(13)	90.6 (3)	O(4)′–Mo(1)′–N(18)′	88.5 (3)
O(5)–Mo(1)–N(18)	85.0 (3)	O(5)′–Mo(1)′–O(6)′	89.3 (3)
O(5)–Mo(1)–O(6)	85.9 (3)	O(5)′–Mo(1)′–O(13)′	158.7 (3)
O(5)–Mo(1)–O(13)	155.3 (3)	O(5)′–Mo(1)′–N(18)′	83.3 (3)
O(5)–Mo(1)–N(18)	84.3 (3)	O(6)′–Mo(1)′–O(13)′	74.60 (26)
O(6)–Mo(1)–O(13)	74.05 (26)	O(6)′–Mo(1)′–N(18)′	81.70 (28)
O(6)–Mo(1)–N(18)	79.8 (3)	O(13)′–Mo(1)′–N(18)′	80.7 (3)
O(13)–Mo(1)–N(18)	78.2 (3)	O(3)′–Mo(2)′–O(24)′	101.0 (3)
O(3)–Mo(2)–O(24)	100.8 (3)	O(3)′–Mo(2)′–O(25)′	99.2 (3)
O(3)–Mo(2)–O(25)	100.7 (3)	O(3)′–Mo(2)′–O(26)′	97.7 (3)
O(3)–Mo(2)–O(26)	91.4 (3)	O(3)′–Mo(2)′–O(33)′	86.95 (27)
O(3)–Mo(2)–O(33)	88.9 (3)	O(5)′–Mo(2)′–N(38)′	172.5 (3)
O(24)–Mo(2)–N(38)	170.8 (3)	O(24)′–Mo(2)′–O(25)′	106.7 (3)
O(24)–Mo(2)–O(25)	107.0 (3)	O(24)′–Mo(2)′–O(26)′	90.0 (3)
O(24)–Mo(2)–O(26)	89.1 (3)	O(24)′–Mo(2)′–O(33)′	162.7 (3)
O(24)–Mo(2)–O(33)	161.2 (3)	O(24)′–Mo(2)′–N(38)′	85.0 (3)
O(24)–Mo(2)–N(38)	84.7 (3)	O(25)′–Mo(2)′–O(26)′	153.4 (3)
O(25)–Mo(2)–O(26)	157.5 (3)	O(25)′–Mo(2)′–O(33)′	86.9 (3)
O(25)–Mo(2)–O(33)	86.7 (3)	O(25)′–Mo(2)′–N(38)′	83.1 (3)
O(25)–Mo(2)–N(38)	84.6 (3)	O(26)′–Mo(2)′–O(33)′	73.65 (26)
O(26)–Mo(2)–O(33)	74.47 (26)	O(26)′–Mo(2)′–N(38)′	77.7 (3)
O(26)–Mo(2)–N(38)	81.23 (28)	O(33)′–Mo(2)′–N(38)′	86.05 (27)
O(33)–Mo(2)–N(38)	83.88 (28)	Mo(1)–O(3)–Mo(2)	168.7 (4)
O(3)′–Mo(1)′–O(4)′	101.4 (3)		

Interplanar interactions range from weak, with interplanar separations >3.5 Å, to strong, showing interplanar separations as small as 3.2 Å.[5b,38b] The interplanar distances for $[Mo_2O_5(O_2C_6Cl_4)_2(py)_2]^{2-}$ have a minimum of 3.34 Å and an average value of 3.43 Å. This is well within the range for at least a weak interaction. Thus, it can be envisioned that the tetrachlorocatecholate interligand interactions are responsible for the eclipsed nature of the dianion.

Concluding Remarks. The reactions between $M_2(OR)_6$ compounds (M = Mo and W and R = *i*-Pr and *neo*-Pe) and *o*-quinones give initially $M_2(OR)_6(O\frown O)_2$ compounds, which react further, giving the products $M_2(OR)_4(O\frown O)_3$ and $M_2(OR)_2(O\frown O)_4$. Though only certain members of this series of compounds have been fully characterized, the data are sufficient to formulate all as edge-shared d^1–d^1 M_2O_{10} compounds. The $O\frown O$ ligand is in its fully reduced form and shows a preference to be terminally bound with the bridging positions being occupied by OR ligands. The distortions within the edge-shared M_2O_{10} bioctahedron can be understood in terms of the formation of (i) a M–M σ-bond and (ii) selective axial O-to-M π-bonding.

The reactions involving $M_2(O\text{-}t\text{-}Bu)_6$ take a rather different course. No simple adducts have been isolated or detected but rather a product containing a $[(cis\text{-}MoO_2)_2O]^{2+}$ core. It is tempting to relate the markedly different chemistry observed for R = *t*-Bu relative to that for R = *i*-Pr and *neo*-Pe to a different mechanism for oxidation of the $(M{\equiv}M)^{6+}$ unit. For the bulky R = *t*-Bu, outer electron transfer may occur, leading to $Mo_2(O\text{-}t\text{-}Bu)_6^+$, which decomposes rapidly. Electrochemical oxidation and oxidation by Ag^+ or NO^+ in the presence of pyridine has been found to cause complete loss of alkoxy groups with formation of *trans*-$[Mo(O)(OH)(py)_4]^+$ salts.[44] For the compounds where R = *i*-Pr and *neo*-Pe, where Lewis base association reactions are well-documented, then association of the *o*-quinone with simultaneous or subsequent electron transfer is possible. In view of the apparent coordinative saturation of the compounds $M_2(OR)_6(O\frown O)_2$ and $M_2(OR)_4(O\frown O)_3$ and yet their ease of reaction with *o*-quinones, outer-sphere electron transfer would seem plausible and may well be responsible for decomposition of the alkoxy ligands at the dinuclear center. These questions remain points for future research.

Acknowledgment. We thank the Office of Naval Research and the Wrubel Computing Center for support.

Registry No. **1**, 113598-83-7; **2**, 113598-84-8; **3**, 113598-85-9; **4**, 113598-86-0; **5**, 113598-87-1; **6**, 113598-88-2; **7**, 113598-89-3; **8**, 113598-90-6; **9**, 113598-91-7; **9**·2THF, 113666-76-5; **10**, 113598-92-8; **11**, 113627-34-2; **12**, 113598-93-9; **13**, 113598-95-1; **14**, 113598-96-2; $Mo_2(O\text{-}i\text{-}Pr)_6$, 62521-20-4; $Mo_2(O\text{-}neo\text{-}Pe)_6$, 62521-24-8; $Mo_2(O\text{-}i\text{-}Pr)_8$, 66526-46-3; $Mo_2(O\text{-}i\text{-}Bu)_6$, 51956-21-9; Mo, 7439-98-7; tetrachloro-1,2-benzoquinone, 2435-53-2; 9,10-phenanthrenequinone, 84-11-7.

Supplementary Material Available: Listings of anisotropic thermal parameters, all bond distances and bond angles, and selected least-squares planes and distances of various atoms from these planes (38 pages); listings of F_o and F_c values (101 pages). Ordering information is given on any current masthead page.

(44) Chisholm, M. H.; Huffman, J. C.; Rampulla, R., results to be submitted for publication.